Biochemical and Biophysical Research Communications 407 (2011) 491–494

Contents lists available at ScienceDirect

Biochemical and Biophysical Research Communications

journal homepage: www.elsevier.com/locate/ybbrc

Telomerase inhibition promotes an initial step of cell differentiation of primate embryonic stem cell

Toyoki Maeda [a,*], Ryo Kurita [b], Tomoko Yokoo [b], Kenzaburo Tani [b], Naoki Makino [a]

[a] The Division of Clinical Gerontology, The Department of Molecular and Cellular Biology, Medical Institute of Bioregulation, Kyushu University, Japan
[b] The Division of Clinical Genetics, The Department of Molecular Genetics, Medical Institute of Bioregulation, Kyushu University, Japan

ARTICLE INFO

Article history:
Received 4 March 2011
Available online 15 March 2011

Keywords:
Telomerase
Embryonic stem cell
Marmoset
Cell differentiation

ABSTRACT

Embryonic stem (ES) cell is well known as a totipotent cell, which is derived from a blastcyst and has potential to differentiate into every kind of somatic cell. ES cell bears self-renewal characteristic as well as differentiation potential. ES cell bears telomerase activity to avoid telomere shortening, which is a characteristic of differentiated somatic cells. As the differentiation of ES cells proceeds, their telomerase activity is losing. However, it has not been convinced whether suppression of the telomerase activity promotes progression of ES cell differentiation. The effect of telomerase inhibitor on the differentiation potential of marmoset ES cell was assessed, counting cells expressing embryonic markers (alkaline phosphatase and TPA-1-60) under existence of a telomerase inhibitor. Telomerase inhibitor showed a promotional effect for the marmoset ES cell differentiation. This result suggests that exogenous inhibition of telomerase activity leads to induction of an early differentiation of primate ES cell.

1. Introduction

Stem cell is a totipotent cell which bears potential to differentiate into all kinds of cell type without losing the mitotic activity [1,2]. The stem cells are harbored in all kinds of tissues through the lifetime. They bear also self-renewal potential and keep telomerase activity to prevent telomere shortening resulting from incomplete DNA duplication at every cell division. Embryonic stem (ES) cells are totipotent cells derived from the inner cell mass (ICM) of preimplantation mammalian embryos. They have been used as a suitable material to study cell differentiation at a very early stage and the potential of self-renewal. Stem cell including ES cell is losing its telomerase activity, as its differentiation proceeds. Moreover, immature undifferentiated cell bears a certain telomerase activity and is losing it with differentiating into a mature differentiated cell type. Several undifferentiated cancer cell lines also show the similar behavior, when they are induced to differentiate into more mature cell types [3,4]. These reports have indicated that a mechanism progressing cell differentiation suppresses the telomerase activity. Thus, several reports have shown that exogenous induction of cell differentiation leads to lose the telomerase activity. However, it is controversial about the effect of telomerase activity on cell differentiation. Ectopic telomerase expression in mouse ES cell does not affect cell differentiation [5]. Telomerase down-regulation does not mediate differentiation of a neoplastic cell line PC-12 induced by cytokine [6]. However, chemical inhibition of telomerase activity of myoblast induces expression of differentiation marker protein alpha-smooth muscle actin [7]. On the other hand, ectopic telomerase expression inhibits neuronal differentiation of NT2 neural progenitor cells. [8]. Thus, the effect of telomerase inhibition on cell differentiation seemed inconsistent in previous reports. And few reports have described about this effect for human or primate ES cells. Embryonic stem cells (ESCs) are derived from preimplantation embryos. The common marmoset (*Callithrix jacchus*) is a New World primate species. Thomson et al. [9] established pluripotent common marmoset cell lines, which are considered powerful tools for understanding the regulatory mechanisms of ESC differentiation both in vitro and in vivo. Here, we decided to examine effect of telomerase inhibition on marmoset ES cell differentiation at an initial stage.

2. Materials and methods

2.1. Culture of CMESC Lines

The CM (*cj11*) ESC lines were purchased from the American Type Culture Collection (Manassas, VA, http://www.atcc.org) and WiCell Research Institute, Inc. (Madison,WI, http://www.wicell.org). The CMESC cells were cultured using CMESC medium that consisted of 80% Knockout DMEM supplemented with 20% Knockout Serum Replacement (KSR; Invitrogen), 1 mM L-glutamine,

* Corresponding author. Address: The Division of Clinical Gerontology, The Department of Molecular and Cellular Biology, Medical Institute of Bioregulation, Kyushu University, Beppu, Oita 874-0838, Japan. Fax: +81 977 27 1682.
E-mail address: maedat@beppu.kyushu-u.ac.jp (T. Maeda).

0006-291X/$ - see front matter © 2011 Elsevier Inc. All rights reserved.
doi:10.1016/j.bbrc.2011.03.044

0.1 mM MEM nonessential amino acids, 0.1 mM β-mercaptoethanol (2-ME; Sigma), 100 IU/ml penicillin, 100 μg/ml streptomycin sulfate, 250 ng/ml amphotericin B, as described previously [10]. For cell splitting, undifferentiated CMESC colonies were detached from the feeder cells, using 0.25% trypsin that was supplemented with 1 mM CaCl2 and 20% KSR. The removed colonies were mechanically dissociated into a single cell. After dissociation in 0.25% trypsin/1 mM EDTA, undifferentiated ESCs cultured on irradiated (40 Gy) mouse embryonic fibroblast cell layer were seeded onto low cell-binding dishes (Nalge Nunc, Naperville, IL, http://www.nuncbrand.com) at 0.5–5 × 10^5 cells per 9 cm plate. Similar to other primate ESCs, CMESCs differentiate spontaneously during culturing on MEF feeder layer [11,12]. Cell differentiation of CMESC is induced, especially when the passage period is longer than one day. So, to induce slower differentiation, the medium was changed every day, and we observed a slow spontaneous differentiation.

2.2. Telomerase inhibition

Dissociated single cell suspension was divided into two groups. One was for culture in medium containing a selective G-quadruplex intercalating telomerase inhibitor, 2,6-bis[3-(*N*-Piperidino)propionamido] anthracene-9,10-dione (PPA) at 10 μM for 4 days with daily renewal of culture medium containing the TI. The other was cultured in telomerase inhibitor negative medium as control group. There have been some reports describing the inhibitory effect of the telomerase inhibitor (TI) on telomerase in cell culture condition at the concentration of 10 μM. We chose this concentration for efficient telomerase inhibition and ignorable cytotoxicity in this study [13,14].

2.3. Characterization of differentiated CMESC Lines

To evaluate the differentiated status of the CMESCs, the cells were examined for the expression of embryonic cell markers that are specific for undifferentiated ESCs. The cell lines have been reported to show alkaline phosphatase activity and express TRA-1-60 and lose the phenotype during differentiation [15]. After the 4-day-culture, the cells were harvested and were subjected to immunostaining. To examine the expression of cell surface markers on cultured CMESC, alkaline phosphatase was detected using the Alkaline Phosphatase Staining Kit (Sigma) according to the manufacturer's instructions. For immunostaining, ESCs were fixed with 4% paraformaldehyde in phosphate-buffered saline (PBS) for 10 min at room temperature and then incubated with 0.3% H2O2 for 10 min at room temperature. The primary antibody against an embryonic antigen TRA-1-60 (Chemicon, Temecula, CA, http://www.chemicon.com) was diluted with Antibody Diluent (DAKO ChemMate; DakoCytomation, Glostrup, Denmark, http://www.dakocytomation.dk) and incubated for 1 h at room temperature. Anti-TRA-1-60 (10 μg/ml) as the primary antibody was used. After three washes with PBS, the biotinylated secondary antibody Simple Stain PO Multi system (Nichirei Corporation, Tokyo, http://www.nichirei.co.jp/english) was incubated with the cells for 30 min at room temperature. The samples were washed three times with PBS, and the localization of the bound monoclonal antibodies was detected using the DAB (3,3′-diaminobenzidine tetrahydrochloride) horseradish peroxidase complex. The number of marker positive cells in each colony was counted and the percentage of the positive cells in all the cells in the colony was calculated.

2.4. Telomerase activity

Telomerase activity was determined using the TRAPEZE Telomerase Detection Kit (Chemicon, Tokyo) according to the manufacturer's instructions. Briefly, cell extracts were obtained from approximately 1 × 10^5 cells, and the protein concentrations were measured. Heat-inactivated controls were obtained by incubating the samples at 85 °C for 10 min. Aliquots (1.5 μg) of the cell extracts were used for polymerase chain reaction (PCR), which was performed according to the manufacturer's instructions. The PCR products were electrophoresed on a 1.0% agarose gel, and telomerase activity was detected by ethidium bromide staining.

2.5. Statistics

Mann Whitney Wilcoxon test was used to examine statistical significance of TI-effects on ES cell differentiation. Data are expressed as mean ± S.D. for three replicate experiments. The criterion for the significance is $p < 0.05$. All analysis was carried out using Sigma Statistical Analysis Soft ware (Sigma 2.03, 2001; Sigma, St. Louis, MO).

3. Results

The period of the differentiation is roughly inferred by a percentage of undifferentiated embryonic marker-bearing cells in a colony. If the differentiation occurs before the first cell division, none of cells in the resultant colony would be embryonic marker-positive. The differentiation after the first cell division would result in half of embryonic marker-positives in a colony. If it occurs after the second or later cell division, the colony should contain three quarters or more positive cells. Thus, the percentage of embryonic marker positive cell in a colony indicates roughly the numbers of cell division before the initial differentiation process occurs, as follows: 75–100% for 2 or more cell divisions, 50–75% for 1 or 2, 0–50% for 0 or 1, and 0% for 0. Of course this rough rule could be adapted at most until several cycles of mitosis, because the interval period of mitosis would be different between a differentiated cell and an undifferentiated cell, and because differentiation undifferentiated cells in a colony also proceeds. The initial differentiation process of primate ES cell is detected by the lost expression of embryonic markers, such as alkaline phosphatase and TRA-1-60 [15]. Some representative colonies containing ALP(+) cells or TRA-1-60(+) cells are shown in Fig. 1. Most of cells differentiated into embryonic marker-negative cells and a few percent of colonies remained undifferentiated in the 4-day-culture both in TI(−) and TI(+). TI turned out to promote the cell differentiation, which was detected by counting embryonic marker-expressing cells in ES colonies. The differentiation tendency of ES of each experiment set was various both under TI(−) and TI(+) condition (Table 1). The degree of differentiation induction was also various (30~70% comparing to TI(−)) even under a single set of TI concentration (Table 2). Thus, the initial differentiation process seemed to be delicate and easily affected by subtle fluctuations of the experimental conditions. Even so, the results showed a robust differentiation-promoting effect of TI on ESCs (Table 2, and Fig. 2).

The telomere repeat amplification protocol (TRAP) assay showed that the ES cells under TI(+) condition bore slightly lower telomerase activity comparing to those under TI(−) condition. TI suppressed ~20% of telomerase activity of ES (Fig. 3). The TI at 10 μM suppressed telomerase activity partially. And, even such an incomplete telomerase suppression turned out to be able to promote very early cell differentiation.

4. Discussion

The effect of TI on cell differentiation of various cells was not consistent in past reports. Such a variation of effect of up- or

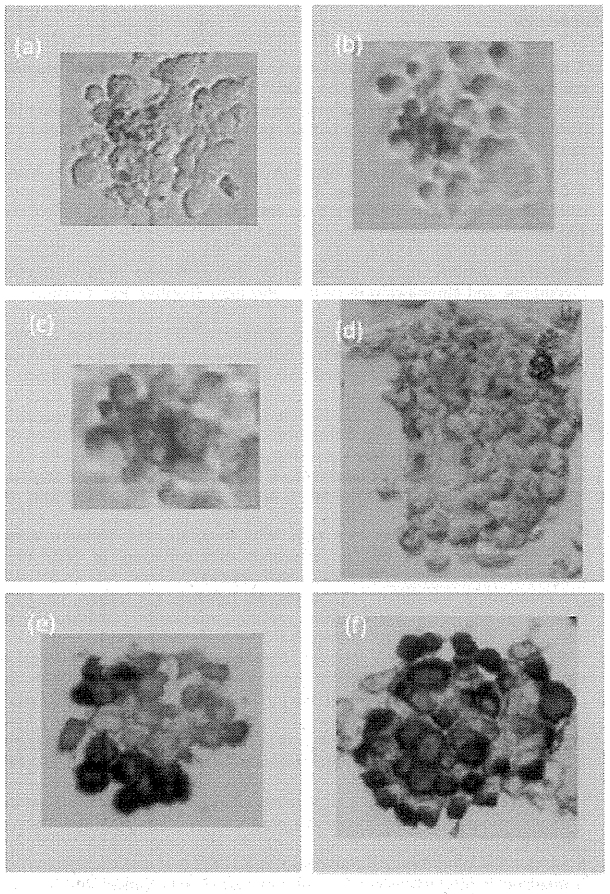

Fig. 1. The detection of differentiation-associated marker-positive and -negative cells in colonies. (A)–(D) Alkaline phosphatase (ALP) positive cells are detected in colonies. The positive cells appear as dark cells or cells bearing black dots. A colony contains less than 25%(A), about 25%(B), about 50%(C), and 100% (= undifferentiated)(D) ALP positive cells. (E) and (F) TRA-1-60 positive cells are dark cells in colonies. A colony contains 50%(E) and 75%(F) TRA-1-60 positive cells.

Table 1
Analysis of percentage of embryonic marker-negative clones in colony.

Marker (experiment set)	ALP(1)		ALP(2)		ALP(3)		TRA-1-	
Negatives in a colony (%)	TI(−)	TI(+)	TI(−)	TI(+)	TI(−)	TI(+)	TI(−)	TI(+)
100	91.3	94.9	74.3	82.4	86.7	95.2	72.9	81.7
50 ≪ 100	7.7	1.8	25.7	11.7	10.1	4.0	25.9	17.3
25 ≪ 50	1.0	2.2	0	4.1	2.6	0.8	0	0
0 ≪ 25	0	0.7	0	0.6	0.6	0	0	0
0 (=100% positive)	0	0.4	0	1.2	0	0	1.2	1.0

TI: Telomerase inhibitor. The numbers of the examined colonies are as follows: 70 for ALP(1) TI(−), 171 for ALP(1) TI(+), 208 for ALP(2) TI(−), 273 for ALP(2) TI(+), 308 for ALP(3) TI(−), 252 ALP(3) TI(+), 85 for TRA-1-60 TI(−), 104 for TRA-1-60 TI(+).

down-regulation of telomerase on cell differentiation might depend on species, cell types, cell differentiation stage, and different experimental procedures for telomerase stimulation or inhibition. ALP and TRA-1-60 are embryonic markers which cells bear only at an initial stage of primate cell differentiation, and usually after the undifferentiated cell such as ESC starts cell differentiation physiologically, the expression of these embryonic markers are losing soon. To analyze the effect for initial cell differentiation of primate, we studied the effect of chemical telomerase inhibition on a

Table 2
The comparison of the proportion of marker positive (= undifferentiated) colonies after 4-day-culure between with and without telomerase inhibitor.

Telomerase inhibitor	(−)	(+)	(+)/(−)
ALP(1)	25.7	17.6	0.685
ALP(2)	8.7	5.1	0.586
ALP(3)	14.3	4.8	0.336
TRA-1-60	27.1	18.3	0.675

The experiment set numbers are parenthesed in the ALP experiments.

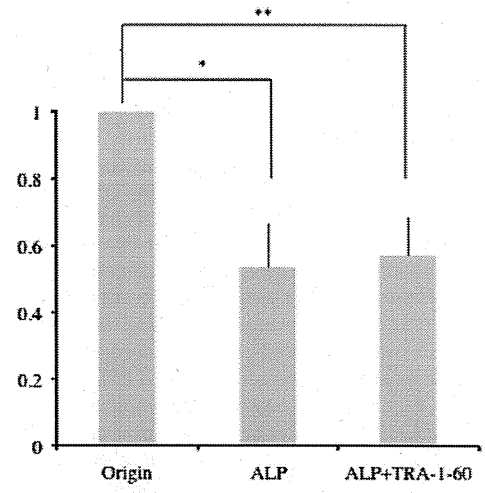

Fig. 2. The ratio of undifferentiated clones in TI(+) to those in TI(−). $^{*}p = 0.047$, $^{**}p = 0.013$.

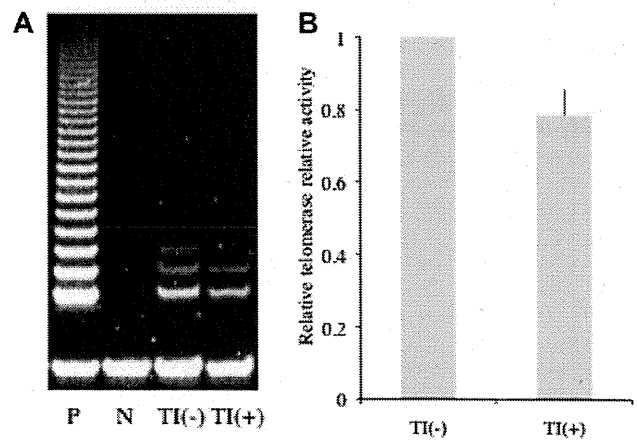

Fig. 3. Comparison of the telomerase activity of cultured CMESCs with and without telomerase inhibitor. (A) A representative result of TRAP assay of CMESCs is shown. A sample for positive control (P) was equipped with the used kit. A heat-inactivated sample was used as negative control (N). (B) The mean proportional telomerase activity of CMESC with telomerase inhibitor is shown, when that without TI is put as one. Horizontal bar depicts standard deviation.

very early differentiation step of primate embryonic stem cell. This report is characterized by treating a primate cell as material and by analyzing an initial stage of cell differentiation. A telomerase inhibitor with G-quadruplex structure has not been reported to affect ESC differentiation. In the present study, CMESCs with TI treatment gave rise to more differentiated colonies containing 0% or <50% embryonic marker positive cells, suggesting that telomerase inhibition lead to promote a primate ES cell differentiation. Our case

is a first report of differentiation of primate ES cell induced by chemical inhibition of telomerase. This seemed to be similar to a previously reported case of chemical induction of myoblast differentiation [7]. However, our results did not seem to be explained by a simple differentiation promotion, because less differentiating (>75% embryonic marker-positive) colonies and colonies consisting of 100%-undifferentiated cells were observed rather in the TI(+) than in the TI(−). This implies that the TI-effect on the differentiation process of ES cell is not always promotional. A very few ES cells might remain undifferentiated and all others might be promoted to differentiate in TI(+) condition. The cellular mechanism of this stem cell heterogeneity of response to telomerase inhibition is unclear. The effects of telomerase inhibition on early cell differentiation process may be much more complicated than having been expected. Such a finding implicated that there are two types of CMESC with telomerase inhibition, one of which was forced to remain in undifferentiated stage, and the other of which was promoted to differentiate into further stages, as the effect of telomerase inhibition on cells depended on the cell type. The two groups would be divided by unknown mechanism, if it exists. Our observation could be a pivotal step for elucidation of the cell differentiation mechanism. The analyzed cell population consisted mainly of embryonic marker-negative differentiated cells, whose telomerase activity had been lowered during the past differentiation process. So, 4-day-cultured CMESC showed a weak telomerase activity, which had been lowered during cell differentiation. TI at a concentration used in this study reduced significantly the telomerase activity of CMESC colonies to ~80% of that of control colonies. Such a mild telomerase inhibition inducing a pivotal step of ESC differentiation may lead to a controllable faster induction of stem cell differentiation, which would be beneficial for regenerative therapy. Further investigation is necessary to reconfirm and analyze the observed phenomenon, using different kinds of stem cells and various methods for telomerase inhibition not only by chemical agents but also by cytogenetical manipulations.

Acknowledgment

This work was supported, in part, by a Grant-in-Aid from the Ministry of Education, Science, and Culture of Japan (#20590703).

References

[1] T. Miura, M.P. Mattson, M.S. Rao, Cellular lifespan and senescence signaling in embryonic stem cells, Aging Cell 3 (2004) 333–343.
[2] S. Wang, C. Hu, J. Zhu, Transcriptional silencing of a novel hTERT reporter locus during in vitro differentiation of mouse embryonic stem cells, Mol. Biol. Cell 18 (2007) 669–677.
[3] H.W. Sharma, J.A. Sokoloski, J.R. Perez, J.Y. Maltese, A.C. Sartorelli, C.A. Stein, G. Nichols, Z. Khaled, N.T. Telang, R. Narayanan, Differentiation of immortal cells inhibits telomerase activity, Proc. Natl. Acad. Sci. USA 92 (1995) 12343–12346.
[4] A.J. Cheng, S.K. Liao, S.E. Chow, J.K. Chen, T.C. Wang, Differential inhibition of telomerase activity during induction of differentiation in hematopoietic, melanoma, and glioma cells in culture, Biochem. Biophys. Res. Commun. 237 (1997) 438–444.
[5] M.K. Lee, M.P. Hande, K. Sabapathy, Ectopic mTERT expression in mouse embryonic stem cells does not affect differentiation but confers resistance to differentiation- and stress-induced p53-dependent apoptosis, J. Cell Sci. 118 (2005) 819–829.
[6] H. Li, A.R. Pinto, W. Duan, J. Li, B.H. Toh, J.P. Liu, Telomerase down-regulation does not mediate PC12 pheochromocytoma cell differentiation induced by NGF, but requires MAP kinase signalling, J. Neurochem. 95 (2005) 891–901.
[7] T. Liu, B. Hu, M.J. Chung, M. Ullenbruch, H. Jin, S.H. Phan, Telomerase regulation of myofibroblast differentiation, Am. J. Respir. Cell Mol. Biol. 34 (2006) 625–633.
[8] R.M. Richardson, B. Nguyen, S.E. Holt, W.C. Broaddus, H.L. Fillmore, Ectopic telomerase expression inhibits neuronal differentiation of NT2 neural progenitor cells, Neurosci. Lett. 421 (2007) 168–172.
[9] J.A. Thomson, J. Kalishman, T.G. Golos, M. Durning, C.P. Harris, J.P. Hearn, Pluripotent cell lines derived from common marmoset (*Callithrix jacchus*) blastocysts, Biol. Reprod. 55 (1996) 254–259.
[10] R. Kurita, E. Sasaki, T. Yokoo, et al., Tal1/Scl Gene transduction using a lentiviral vector stimulates highly efficient hematopoietic cell differentiation from common marmoset (*Callithrix jacchus*) embryonic stem cells, Stem Cells 24 (2006) 2014–2022.
[11] B.E. Reubinoff, M.F. Pera, C.Y. Fong, et al., Embryonic stem cell lines from human blastocysts: somatic differentiation in vitro, Nat. Biotechnol. 18 (2000) 399–404.
[12] H. Suemori, T. Tada, R. Torii, et al., Establishment of embryonic stem cell lines from cynomolgus monkey blastocysts produced by IVF or ICSI, Dev. Dyn. 222 (2001) 273–279.
[13] E. Izbicka, R.T. Wheelhouse, E. Raymond, et al., Effects of cationic porphyrins as G-quadruplex interactive agents in human tumor cells, Cancer Res. 59 (1999) 639–644.
[14] M.A. Shammas, R.J. Shmookler Reis, C. Li, et al., Telomerase inhibition and cell growth arrest by G-quadruplex interactive agent in multiple myeloma, Mol. Cancer Ther. 2 (2003) 825–833.
[15] E. Sasaki, K. Hanazawa, R. Kurita, et al., Establishment of novel embryonic stem cell lines derived from the common marmoset (*Callithrix jacchus*), Stem Cells 23 (2005) 04–13.

SCIENTIFIC REPORTS

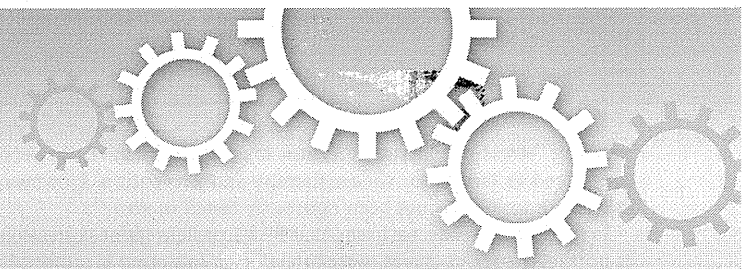

OPEN

SUBJECT AREAS:
CANCER
CANCER MODELS
CELL DEATH
ONCOGENESIS

Received
22 February 2011

Accepted
25 March 2011

Published
14 June 2011

Correspondence and requests for materials should be addressed to A.T. (atsushit@sentan.med.kyushu-u.ac.jp)

* deceased

A novel potent tumour promoter aberrantly overexpressed in most human cancers

Atsushi Takahashi[1,2,4], Hisashi Tokita[3]*, Kenzo Takahashi[5], Tomoharu Takeoka[4], Kosho Murayama[1], Daihachiro Tomotsune[2], Miki Ohira[2], Akihiro Iwamatsu[6], Kazuaki Ohara[7], Kazufumi Yazaki[7], Tadayuki Koda[8], Akira Nakagawara[2] & Kenzaburo Tani[1]

[1]Division of Molecular and Clinical Genetics, Department of Molecular Genetics, Medical Institute of Bioregulation, Kyushu University, Fukuoka 812-8582, Japan, [2]Division of Biochemistry and [3]Division of Animal Science, Chiba Cancer Center Research Institute, Chiba 260-8717, Japan, [4]Department of Hematology and Oncology and [5]Department of Dermatology, Graduate School of Medicine, Kyoto University, Kyoto 606-8507, Japan, [6]Protein Research Network, Inc., Yokohama, Kanagawa 236-0004, Japan, [7]Laboratory of Plant Gene Expression, Research Institute for Sustainable Humanosphere, Kyoto University, Uji 611-0011, Japan, [8]Hisamitsu Pharmaceutical Co., Inc., Tokyo 100-6221, Japan.

The complexity and heterogeneity of tumours have hindered efforts to identify commonalities among different cancers. Furthermore, because we have limited information on the prevalence and nature of ubiquitous molecular events that occur in neoplasms, it is unfeasible to implement molecular-targeted cancer screening and prevention. Here, we found that the FEAT protein is overexpressed in most human cancers, but weakly expressed in normal tissues including the testis, brain, and liver. Transgenic mice that ectopically expressed FEAT in the thymus, spleen, liver, and lung spontaneously developed invasive malignant lymphoma (48%, 19/40) and lung-metastasizing liver cancer (hepatocellular carcinoma) (35%, 14/40) that models human hepatocarcinogenesis, indicating the FEAT protein potently drives tumorigenesis *in vivo*. Gene expression profiling suggested that FEAT drives receptor tyrosine kinase and hedgehog signalling pathways. These findings demonstrate that integrated efforts to identify FEAT-like ubiquitous oncoproteins are useful and may provide promising approaches for cost-effective cancer screening and prevention.

Although our understanding of the molecular mechanisms of carcinogenesis has greatly improved, this knowledge has not lead to the identification and development of effective tools for cancer screening and prevention [1]. Approximately 30–40% of all cancer deaths are preventable, and this estimation is based on indirect measures that do not interfere with carcinogenesis, such as dietary modifications, lifestyle changes, minimizing carcinogen exposure, and vaccination against oncogenic viruses [1]. More advanced chemoprevention measures such as tamoxifen, raloxifene, finasteride, and celecoxib [1] and the eradication of *Helicobacter pylori* are only available to high-risk groups for particular cancers.

In order to reach the long-term goal of establishing molecular-targeted cancer screening and prevention, it is important that we explore, characterize, and catalogue a distinct subclass of cancer genes [2] that are involved in diverse cancers. However, the systematic approaches that have been used to identify cancer genes, such as sequencing protein-coding exons [3–9], whole genome sequencing [10,11], and paired-end sequencing to comprehensively identify somatic rearrangements [12], have only further emphasized the marked heterogeneity and complexity of human neoplasms and have not successfully identified commonalities among cancers. Driver mutations that contribute to the development of human cancers [13] are highly variable among different types of cancer and among individual tumours of the same type. Thus, it is still unknown if there are oncogenic molecules that are commonly altered in diverse cancers.

There is accumulating evidence that cancers have heterogeneous combinations of deregulated cancer genes [13,14] and that signalling pathways rather than individual genes are the targets in tumorigenesis [15]. Although some canonical signalling pathways are universally deregulated in cancers, different components of these pathways can be affected in different tumours [3,5–9,15]. The proteins that are commonly overexpressed in cancers are predominantly thought to reflect "peripheral" changes [2,15] that result from neoplastic phenotypes (i.e., augmented metabolic and homeostatic processes such as glycolysis, macromolecular synthesis, and DNA replication) [16,17] and the

resulting "stress phenotype" [18]. Thus, these proteins have not been considered as targets for cancer therapy and prevention. However, this presumption has not been rigorously tested *in vivo* [19].

In the present study, we found that FEAT protein (*f*aint *e*xpression in normal tissues, *a*berrant overexpression in *t*umours) is uniformly overexpressed in a variety of human cancers. Remarkably, FEAT transgenic mice indicated that FEAT potently drives tumorigenesis *in vivo*. Expression microarray analyses suggested that FEAT induces oncogenic pathways. The significance of overexpressed genes in cancer is increasingly recognized as potential leads for a variety of diagnostic and therapeutic approaches [6,7,20]. Additional studies that identify and characterize FEAT-like oncogenic proteins will hopefully advance molecular-targeted cancer screening and prevention.

Results

Biochemical purification of FEAT protein. On analyses of molecules regulating nuclear apoptosis in a cell-free system [21,22], we noticed that the apoptosis-inducing activity was attenuated in the middle of active fractions, concomitant with the appearance of two polypeptides with apparent molecular masses of 74 and 66 kDa (Supplementary Fig. 1). This suggested that apoptosis inhibitors were copurified with apoptosis inducers. Microsequencing revealed that the 74 kDa protein is a rat homologue of human CGI-01 protein [23] that is encoded by *METTL13* (methyltransferase like 13) gene (also known as *KIAA0859*). CGI-01, renamed FEAT, contains two S-adenosylmethionine-binding motifs (SAM-binding motifs) that are characteristic of methyltransferases and related enzymes (see Fig. 1f) [24], and the structure is well conserved across species (Supplementary Fig. 2). Capture compounds mass spectrometry using S-adenosylhomocysteine has detected the *Arabidopsis thaliana* orthologue of FEAT (At2g31740) [25], suggesting that FEAT can bind SAM. We did not detect protein methyltransferase activity, spermidine/spermine synthase activity, or ubiquinone synthase activity (Supplementary Fig. 3) in full-length or truncated FEAT proteins (Supplementary Note). Further

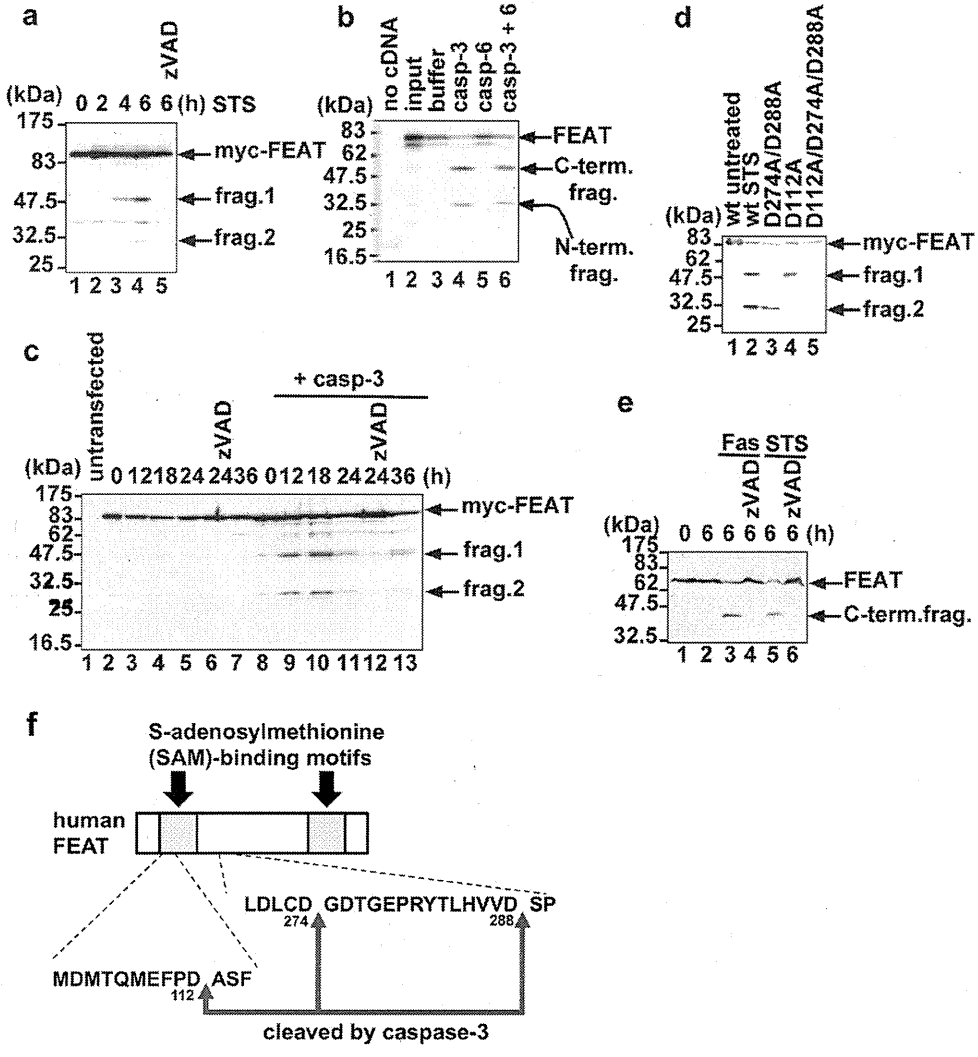

Figure 1 | FEAT is a substrate for caspase-3. (a) Cleavage of N-terminal Myc-tagged FEAT (myc-FEAT) in apoptotic cells. COS-7 cells expressing myc-FEAT were treated with 1 μM staurosporine (STS) for the indicated times. Lane 5: cells pretreated for 30 min with 100 μM zVAD-fmk, a broad spectrum caspase inhibitor. (b) *In vitro* transcribed/translated [^{35}S]-labelled FEAT was cleaved by purified caspase-3, but not by caspase-6. (c) Caspase-3 is mainly responsible for FEAT cleavages. MCF-7 cells expressing myc-FEAT alone or together with procaspase-3 (+ casp-3) were treated with 1 μM STS for the indicated times. (d) Mutating caspase-3 cleavage sites abrogates FEAT cleavages. COS-7 expressing wild-type (wt) or mutant myc-FEAT were treated for 6 h with 1 μM STS (lane 2 to 5). Immunoblots (a, c, d) were probed with an anti-Myc antibody. (e) Cleavage of endogenous FEAT in apoptotic cells. Jurkat T cells preincubated for 1 h without or with 100 μM zVAD-fmk were treated for 6 h with 100 ng/ml CH-11 agonistic anti-Fas antibody or 1 μM STS. The immunoblot was stained with the anti-FEATΔN antibody. (f) Schematic diagram of the human FEAT structure and caspase-3 cleavage sites.

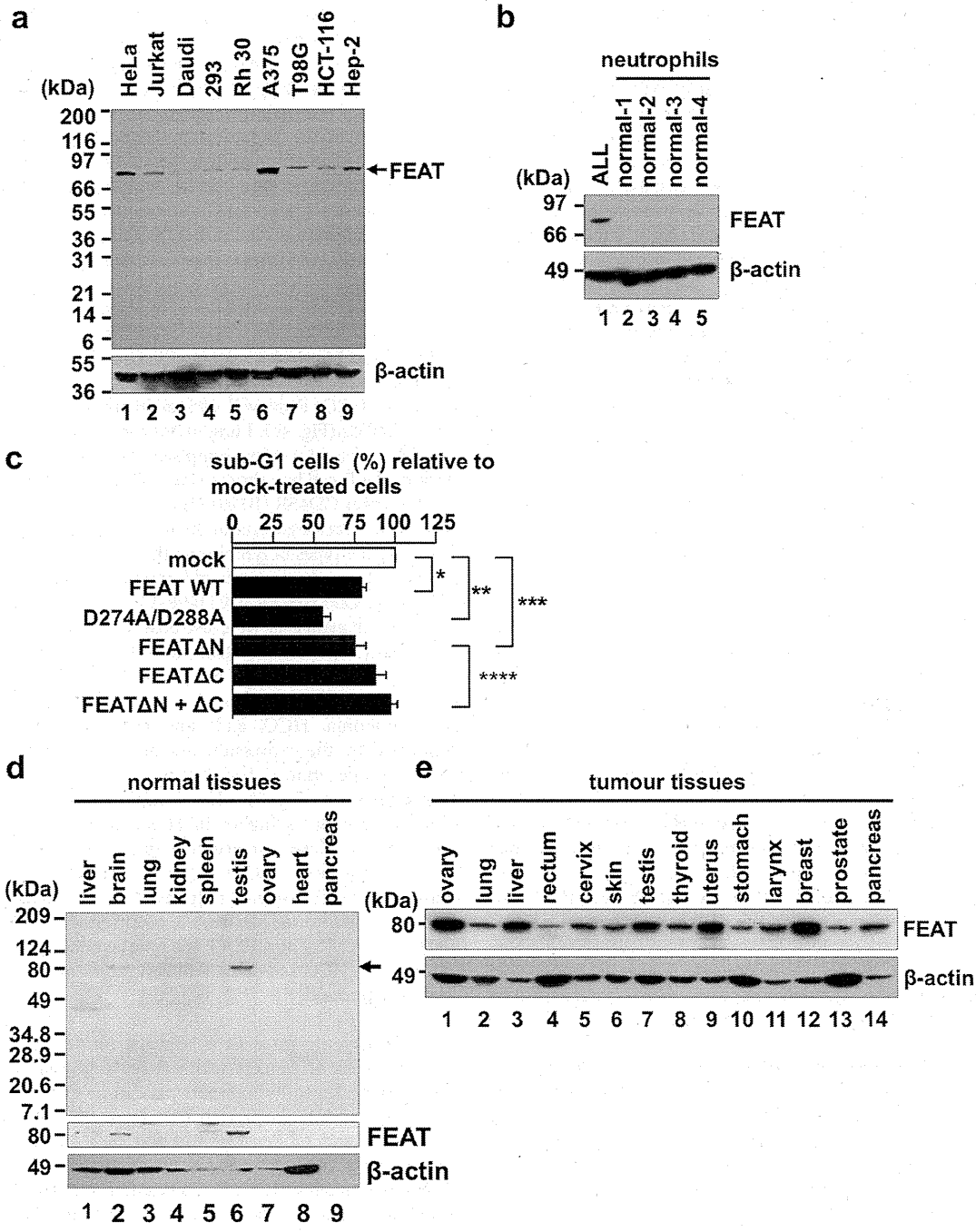

Figure 2 | FEAT is overexpressed in human cancers. (a) The immunoblot (IMB-105) contains lysates (10 μg protein/lane) from the following human cancer-derived cell lines: HeLa, uterine cervical carcinoma; Jurkat, T-cell leukaemia; Daudi, Burkitt lymphoma; 293, embryonal kidney transformed by adenovirus type 5; Rh 30, rhabdomyosarcoma; A375, malignant melanoma; T98G, glioblastoma; HCT-116, colon carcinoma; and Hep-2, larynx carcinoma. Immunofluorescence microscopy using the same antibody revealed that FEAT is diffusely localized in the cytoplasm and nucleus of HeLa cells (Supplementary Fig. 5; Supplementary Note). (b) Absence of FEAT expression in normal neutrophils. Peripheral blood mononuclear cells from a patient with acute lymphoblastic leukaemia (ALL) and neutrophils from four normal volunteers were analyzed by immunoblotting. (c) FEAT attenuates spontaneous neutrophil apoptosis. His-tagged wild-type (WT) or mutant FEAT proteins were introduced into neutrophils by protein transduction. Apoptotic neutrophils with a hypodiploid DNA content were analyzed by flow cytometry and normalized to that of cells incubated with irrelevant proteins (mock) (*, $P = 0.0012$, $n = 9$; **, $P = 0.0001$, $n = 9$; ***, $P = 0.0192$, $n = 4$; ****, $P = 0.0135$, $n = 4$; paired t-test). Error bars, s.e.m. (d) Multiple Tissue Blot (Human, WB46, 75 μg protein/lane) was probed with anti-FEATΔN (uppermost panel; FEAT is indicated by an arrow), anti-FEATΔC (middle panel), and anti-actin (lowermost panel) antibodies. (e) Human Tumor Tissue Blot (WB51). The proteins loaded (50 μg/lane) were derived from the following: ovary stromal sarcoma, lung adenocarcinoma, hepatocellular carcinoma, rectal adenocarcinoma, cervical squamous cell carcinoma, skin malignant melanoma, testis embryonal carcinoma, thyroid follicular carcinoma, uterine adenocarcinoma, stomach adenocarcinoma, laryngopharynx squamous cell carcinoma, breast ductal carcinoma, prostate hyperplasia, and pancreatic adenocarcinoma. (a, b, and e) Blots were probed with anti-FEATΔN (upper panels) and anti-actin (lower panels) antibodies.

studies are required to determine whether FEAT has enzymatic activities.

FEAT is cleaved by caspase-3. Exogenously-expressed FEAT was cleaved during staurosporine-induced (STS-induced) apoptosis of COS-7 cells (Fig. 1a). *In vitro* transcribed/translated FEAT was cleaved by caspase-3, but not by caspase-6 (Fig. 1b). Purified His-tagged FEAT was cleaved by purified caspase-3. FEAT was minimally cleaved in apoptotic MCF-7 cells, which are deficient in caspase-3 [26], and coexpression of procaspase-3 led to efficient cleavages of FEAT (Fig. 1c). Site-directed mutagenesis studies (Fig. 1d) revealed caspase-3 cleavage sites in human FEAT. Endogenous FEAT was cleaved in Jurkat T cells undergoing Fas- and STS-induced apoptosis (Fig. 1e). These results indicated that caspase-3 cleaves FEAT in apoptotic cells (Fig. 1f). D112 and D288 are well conserved across species (Supplementary Fig. 2; Supplementary Note), suggesting that caspase cleavages of FEAT play critical role(s) in organisms.

FEAT attenuates apoptotic cell death and the antiapoptotic activity is abrogated upon caspase-3-mediated cleavages. Cleavages of antiapoptotic kinases and phosphatases by caspases fine-tune apoptosis through terminating prosurvival signalling and generating proapoptotic peptide fragments [27]. We therefore assessed whether FEAT or its caspase-3-cleaved fragments affect apoptosis. *Ex vivo* experiments using plasmid transfection and RNA interference suggested that FEAT can impede apoptosis (Supplementary Fig. 4; Supplementary Note). We searched for cell types that do not express FEAT, found that almost all cancer-derived cell lines express FEAT (Fig. 2a), and decided to use neutrophils (Fig. 2b).

Protein transduction [28] of wild-type FEAT (FEAT WT) and FEATΔN (amino acid 289–699), a fragment generated by caspase-3 cleavage, significantly attenuated spontaneous apoptosis in neutrophils (Fig. 2c). The D274A/D288A mutant was more potent than FEAT WT or FEATΔN. In contrast, FEATΔC (amino acid 1–274), N-terminal fragment generated by the cleavage between the SAM-binding motifs, did not affect apoptosis, and the addition of FEATΔC interfered with the antiapoptotic function of FEATΔN (FEATΔN + ΔC). Taken together, the results are consistent with the notion that FEAT has the ability to attenuate apoptosis, which is abrogated by caspase-3 cleavages between the SAM-binding motifs.

FEAT is aberrantly overexpressed in human cancer tissues. We noticed that FEAT corresponds to the TGACCTCCAG tag that is used in the serial analysis of gene expression (SAGE) studies of human transcriptomes, which has been linked to a transcript that is uniformly elevated in human colon, brain, breast, and lung cancers and melanoma compared with the corresponding normal tissues [29]. Consistent with these classifications, immunoblotting analyses of normal human tissues showed weak FEAT expression only in the testis, brain, and liver (Fig. 2d), which correlated with mRNA expression [23]. In marked contrast, FEAT protein was moderately to highly expressed in a wide range of human cancer tissues (Fig. 2e), suggesting that FEAT is a ubiquitous protein involved in tumour biology.

FEAT upregulation is oncogenic *in vivo*. To assess whether FEAT upregulation in human cancers contributes to tumorigenesis, we generated transgenic mice that express human FEAT under a promoter that is active in a wide range of tissues (Supplementary Note). Immunoblotting showed expression of FEAT in the thymus, spleen, liver, and lung of transgenic mice (Fig. 3a). Thymocytes from transgenic mice showed significant decreases in Fas ligand- and glucocorticoid-induced cell death (Fig. 3b), indicating that transgenic expression of FEAT attenuates apoptosis.

After 12 month of age, the transgenic mice began developing hepatocellular carcinoma (HCC), as supported by immunohistochemical analyses of α-fetoprotein and albumin, and malignant lymphoma (Fig. 3c and Supplementary Fig. 6). HCC was also observed in a 9-month-old male transgenic mouse (Supplementary Fig. 6), suggesting that the hepatocarcinogenesis can be initiated earlier. In contrast, none of the nontransgenic littermates developed HCC, and lymphoma was observed in nontransgenic littermates with a lower incidence (18%, 3/17). Consequently, the transgenic mice developed tumours or died earlier than the nontransgenic littermates (Fig. 4a). HCC and lymphoma were observed in the offspring of four distinct founders (Fig. 3c), arguing against the possibility that the tumorigenesis resulted from integration of the transgene in endogenous cancer genes in the mouse genome. The murine HCC recapitulated the strong male predilection (Fig. 3c) that is observed in human patients [30].

Murine HCCs displayed various histological subtypes similar to human HCCs (Fig. 4b). Lung metastases were detected in two mice with HCC (Fig. 4c). Most lymphomas belonged to diffuse large or Burkitt-like B-cell lymphoma (Fig. 5a), both of which expressed the B-cell marker CD45R (B220) (100%, 15/15) (inset) and had undergone clonal rearrangement of the immunoglobulin genes (83%, 5/6). These are the types of lymphoma that are most common in human patients. None of the examined lymphomas were positive for the T-cell marker CD3 (0%, 0/7). CD45R- and CD3-negative polymorphic variants with giant cells were also observed (Fig. 5b). The lymphomas were highly invasive and often infiltrated the pancreas (Fig. 5c).

One transgenic mouse developed both HCC and lymphoma (Fig. 5d), and another transgenic mouse harboured three tumours, i.e., lymphoma, HCC, and lung adenocarcinoma (Fig. 5e), as confirmed by the expression prosurfactant protein C (insets). In addition, one mouse had lymphoma and rhabdomyosarcoma (Supplementary Fig. 6). Immunohistochemistry showed that FEAT expression is higher in HCCs than adjacent liver tissues. Sequencing analyses showed that there were no mutations in the FEAT transgene in HCCs (0%, 0/5), suggesting that structural changes in FEAT are not required for tumorigenesis. Unlike the CF-1 and C3H inbred strains, the occurrence of HCC is unusual in C57BL/6 mice [31]. Thus, FEAT is a unique oncoprotein that potently induces both HCC and malignant lymphoma on the C57BL/6 inbred strain background.

FEAT transgenic mice as a relevant model for human HCCs. Mouse models of cancers with extensive physiological and molecular similarities to human patients can be exploited to determine the causes of human cancers, to devise the strategy for cancer prevention, and to develop and test new treatments [32]. Inflammation plays critical roles in the initiation and promotion of human and murine HCCs [33]. To evaluate the possibility that FEAT promotes hepatocarcinogenesis by inducing prolonged inflammatory responses such as autoimmune hepatitis, we examined whether FEAT transgenic mice with HCC have background inflammatory lesions in the liver. Only sparse low-grade perivasculitis with minimal tissue destruction was observed in 50% (7/14) of the liver adjacent to HCC in FEAT transgenic mice, while a similar degree of perivasculitis was detected in 35% (6/17) of the liver from nontransgenic littermates (Supplementary Fig. 7). The observations did not support the idea that FEAT causes HCC through inflammatory mechanisms.

We next assessed whether the HCCs in FEAT transgenic mice closely model genetic events in human HCCs. The loss of p53 tumour suppressor function is a key event in certain subsets of human HCCs [34]. In particular, HCCs caused by aflatoxin characteristically have the S376A mutation in p53. Mutations in the open reading frame (ORF) of the p53 mRNA were not detected in mouse HCCs (0%, 0/7). MDM2 amplification, which is observed in some human HCCs [35], was unlikely

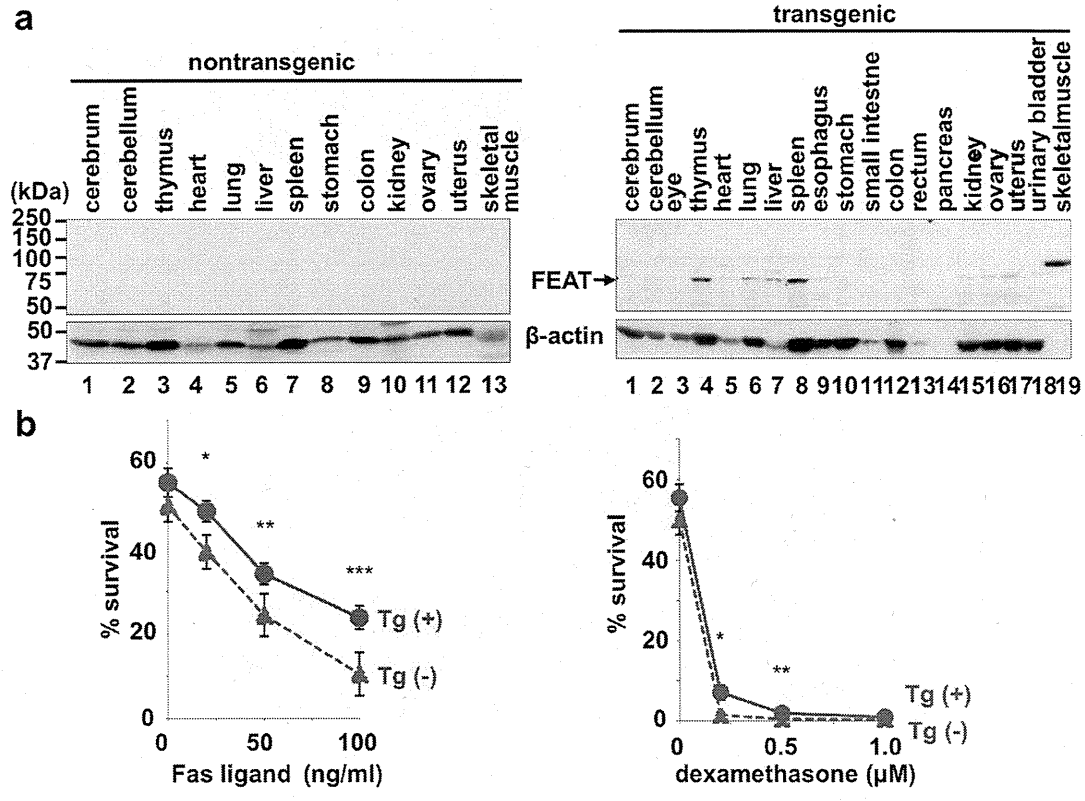

c

mouse lines	1 (n = 7)	10 (n = 1)	14 (n = 1)	16 (n = 12)	18 (n = 12)	23 (n = 7)
age at analyses (months)	9-28	27	28	18-27	12-23	18-30
HCC	3	0	0	4	6	1
lymphoma	1	1	1	5	6	6
other tumour	0	0	0	2	0	1
non-tumour death	3	0	0	2	1	1

	male (n = 26)	female (n = 14)
age at analysis (months)	9-30	17-28
HCC	13 (50%)	1 (7.1%)
lymphoma	10 (38%)	10 (71%)
other tumours	1 (3.8%)	2 (14%)
non-tumour death	5 (19%)	2 (14%)

Figure 3 | Analyses of FEAT transgenic mice. (a) FEAT protein expression in nontransgenic (left panel) or transgenic (right panel) mouse organs. Similar results were obtained with first generation offspring of three distinct founders. The blot (30 μg protein/lane) was probed with anti-FEATΔN (upper panels) and anti-actin (lower panels) antibodies. (b) Cell death of thymocytes is attenuated in FEAT transgenic mice. Survival of thymocytes isolated from transgenic mice (Tg (+)) (red, solid lines) or nontransgenic littermates (Tg (-)) (blue, dashed lines) were analyzed by flow cytometry (means ± s.e.m.) after treatment for 24 h with Fas ligand (left panel) (*, $P = 0.02492$; **, $P = 0.0497$; ***, $P = 0.0226$, $n = 5$; paired t-test) or dexamethasone (right panel) (*, $P = 0.0331$; **, $P = 0.0411$, $n = 6$; paired t-test). (c) Tumours in founder, first and second generation FEAT transgenic mice. HCC, hepatocellular carcinoma.

because immunohistochemistry did not reveal increased MDM2 in the mouse HCCs compared with adjacent normal liver tissues (0%, 0/5). Activation of Wnt signalling pathway through mutations in ß-catenin or Axin that is found in a small population of human HCCs [36] was unlikely because of the absence of the nuclear localization of ß-catenin (0%, 0/6) and of any mutations in the hotspots in the ß -catenin gene (0%, 0/9). Overall, HCCs in the transgenic mice do not correspond to certain minor subsets of human HCCs [36].

To evaluate whether the mouse HCCs harbour chromosomal changes similar to human patients, the amplification (gain) or deletion (loss) of genomic regions (copy number alterations, CNAs) were analyzed by microarray-based comparative genomic hybridization (array-CGH). A genome-wide view of large-scale CNAs showed that the murine HCCs had marked genomic instability, with more gains than losses (Supplementary Fig. 8) as observed in human HCC [37], while the liver from a transgenic mouse without HCC had minimal

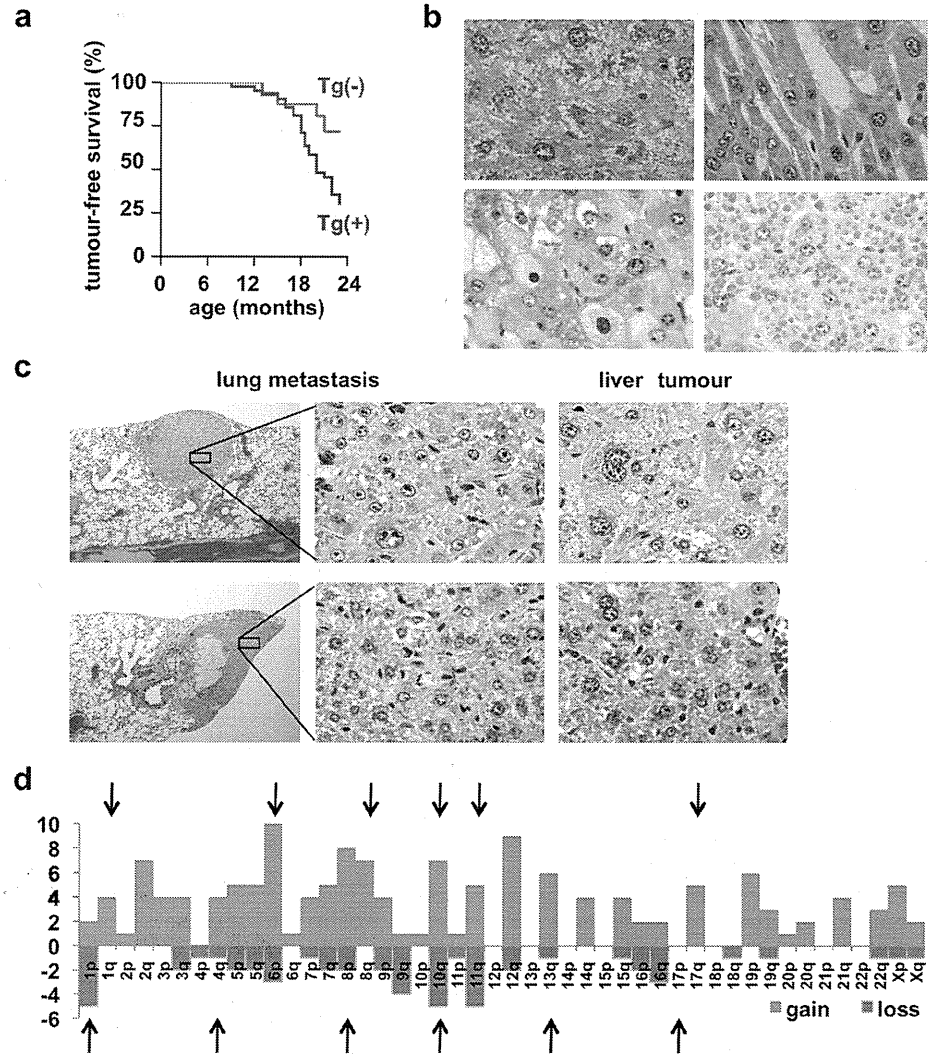

Figure 4 | Hepatocellular carcinoma (HCC) in FEAT transgenic mice. (a) Kaplan-Meier curve for tumour-free survival of FEAT transgenic mice (Tg (+)) (red) ($n = 40$) and nontransgenic littermates (Tg (-)) (blue) ($n = 17$) ($P = 0.038$, log-rank test). (b) Various histological subtypes of HCC. Well-differentiated tumours composed of dysplastic hepatocytes with atypical large polyploid nuclei and anisokaryosis with compact (upper left panel) and trabecular (upper right panel) growth patterns, and variants such as a clear-cell type (left lower panel) and HCCs with cytoplasmic inclusion bodies (right lower panel). (c) Morphology of neoplastic cells in lung metastases, which were similar to primary liver tumours. (b and c) hematoxylin and eosin (H&E) staining. Original magnifications are: ×115 (c, left panels) and ×600 (b; c, middle and right panels). (d) Syntenic human chromosomal regions corresponding to CNAs detected by array comparative genomic hybridization (array-CGH). Each column shows the number of genes present in each human chromosomal arm that was commonly gained (red) or lost (green) in HCCs of FEAT transgenic mice ($n = 6$). The arrows indicate the chromosomal arms that are gained or lost in human HCCs [41].

CNAs. This suggested that genomic fragility developed during the process of hepatocarcinogenesis rather than because of direct effects of the FEAT transgene.

Tandem duplications that range in size from 3 kb to greater than 1 Mb is the most commonly observed architectures of rearrangement in a recent study of human breast cancer genomes [12]. High-resolution array-CGH revealed gain or loss of such small chromosomal segments in the murine HCCs. The small-scale CNAs involved 18 known cancer genes (http://www.sanger.ac.uk/genetics/CGP/Census/) (*MDS1*, *PDGFRA*, *PIK3R1*, *JAZF1*, *WHSC1L1*, *HOOK3*, *PCM1*, *MLLT3*, *PTEN*, *CBL*, *ERCC5*, *ERCC4*, *CYLD*, *CBFB*, *BRIP1*, *MLLT1*, *TMPRSS2*, *NF2*) (Supplementary Table 1). *TTN* [4], *SKP2* [38], *EED1* [39], and *PVT1* [40] have also been implicated in oncogenesis. To directly compare the small-scale CNAs in mouse and human HCCs, we listed focal CNAs that were shared among the murine HCCs and identified human chromosomal loci syntenic to the CNAs (Supplementary Table 1). The syntenic regions covered most of the chromosomal changes that were previously implicated in human HCCs [41] (Fig. 4d) and exhibited marked similarities with array-CGH data of human HCCs [37]. This cross-species synteny implies that the carcinogenesis in these mice closely mimics that in human patients and indicates that the FEAT transgenic mouse may be a highly relevant model of human HCCs [42].

Molecular bases for oncogenic functions of FEAT. The oncogenic potential of FEAT in transgenic mice seemed to be disproportionate to the moderate ability to attenuate apoptosis (Fig. 2c, Fig. 3b, and Supplementary Fig. 4). NIH3T3 cells that overexpressed FEAT, FEATΔN, or FEATΔC did not consistently form colonies in soft agar, suggesting that the assay for anchorage-independent growth can fail to detect potently tumorigenic genes. This supported the limitation of *ex vivo* screening for cancer genes and the much

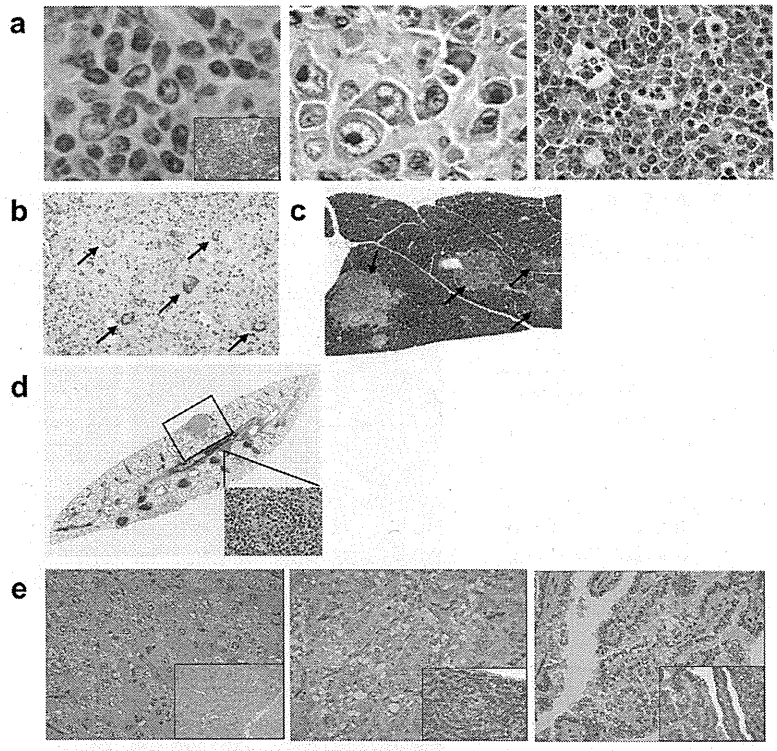

Figure 5 | Lymphoma and co-occurrence of other tumours in FEAT transgenic mice. (a) Microscopic appearance of B-cell lymphomas from FEAT transgenic mice. Centroblastic (left panel) or immunoblastic (middle panel) variants of diffuse large B-cell lymphoma and Burkitt-like B-cell lymphoma with a starry sky appearance (right panel). (b) Giant cells (arrows) in polymorphic lymphoma. (c) Infiltration of lymphoma in the pancreas (arrows). (d) A section of the lung with metastases of hepatocellular carcinoma (HCC) (rectangle, corresponding to left upper panel in Fig. 4c) and lymphoma (inset). (e) HCC (left panel), and a lung adenocarcinoma (middle and right panels) that developed in a transgenic mouse, which also harboured lymphoma. (a–e) H&E staining. Original magnifications are: ×600 (a), ×115 (b), ×60 (c), ×15 (d), and ×400 (e). The insets show immunohistochemical staining for a B-cell marker CD45R (B220) (a), and prosurfactant protein C, a marker of type II pneumocytes, which was absent in the HCC and present in the lung adenocarcinoma (e).

broader relevance of genetic engineering and *in vivo* analyses of mice [19].

To evaluate whether FEAT has cellular functions relevant in oncogenesis, FEAT was overexpressed in NIH3T3 cells, which only weakly express FEAT protein (Fig. 6a), and the alterations in genome-wide transcriptional profiles were analyzed by microarrays. Gene set enrichment analysis (GSEA) [43] revealed that FEAT overexpression increases the signatures of receptor tyrosine kinase (RTK) and hedgehog signalling pathways (Fig. 6b and Supplementary Table 2), which are known to play major roles in the development and maintenance of cancers [44–46]. The results suggested that the ability to drive multiple oncogenic pathways underlies the robust tumorigenic potential of FEAT *in vivo*.

FEAT is upregulated in most human cancer cells. Previous studies using expression microarrays reported that FEAT (KIAA0859, CGI-01) mRNA is upregulated in uterine and ovarian cancers (http://www.freepatentsonline.com/20050244843.html), superficial bladder cancer (https://www.oncomine.org), adenocarcinomas of the stomach [47], and retinoblastoma [48]. To further assess the range of human cancers in which FEAT may be involved in oncogenesis, we examined FEAT levels in various human cancers and their subtypes using Tissue Arrays. Immunohistochemistry detected significant upregulation of FEAT in colon (46%, 17/37), pancreatic (61%, 11/18), prostate (39%, 7/18), breast (51%, 18/35), ovary (24%, 6/25), thyroid (47%, 9/19), and non-small-cell lung cancers (64%, 14/22) (Fig. 7 and Supplementary Fig. 9; Supplementary Table 3). FEAT was upregulated in cancer cells but not nonneoplastic stromal cells or normal cells adjacent to cancer tissues. Thus, FEAT upregulation is common and widespread in human cancers, suggesting that this phenomenon is a fundamental process in the development of most cancers.

Notably, FEAT overexpression can also precede neoplastic transformation in human HCCs; hepatocytes that were adjacent to HCC in liver cirrhosis expressed high levels of FEAT (Fig. 8), most likely reflecting ongoing carcinogenesis in these cirrhotic livers. FEAT overexpression was also observed in intraductal carcinoma *in situ* of breast (Supplementary Fig. 9) [49], an early phase preceding invasion. These observations suggest that FEAT functions from preneoplastic or early neoplastic processes of diverse human cancers.

Discussion

One of the most feasible and promising approaches for cancer prevention and screening is to target a common event that occurs in most tumours. Despite these potential therapeutic advantages, it is still poorly understood whether a crucial molecular event commonly occurs in the early oncogenesis of most cancers. The present study demonstrates that an unrecognized protein, FEAT, is highly oncogenic *in vivo*. Remarkably, this prominent promoter of tumorigenesis is aberrantly overexpressed in most human cancers starting in the early phases of tumorigenesis. Chromatin immunoprecipitation studies with mouse embryonic stem cells (ESCs) indicate that oncogene products such as c-Myc [50–52], N-Myc [51], and E2F1 [51] are bound to the promoter of the mouse *Mettl13* gene (also known as *5630401D24Rik*). Amplicons in various cancers including HCC [37], malignant lymphoma, and high-risk multiple myeloma (http://www.freepatentsonline.com/y2008/0274911.html) involve the

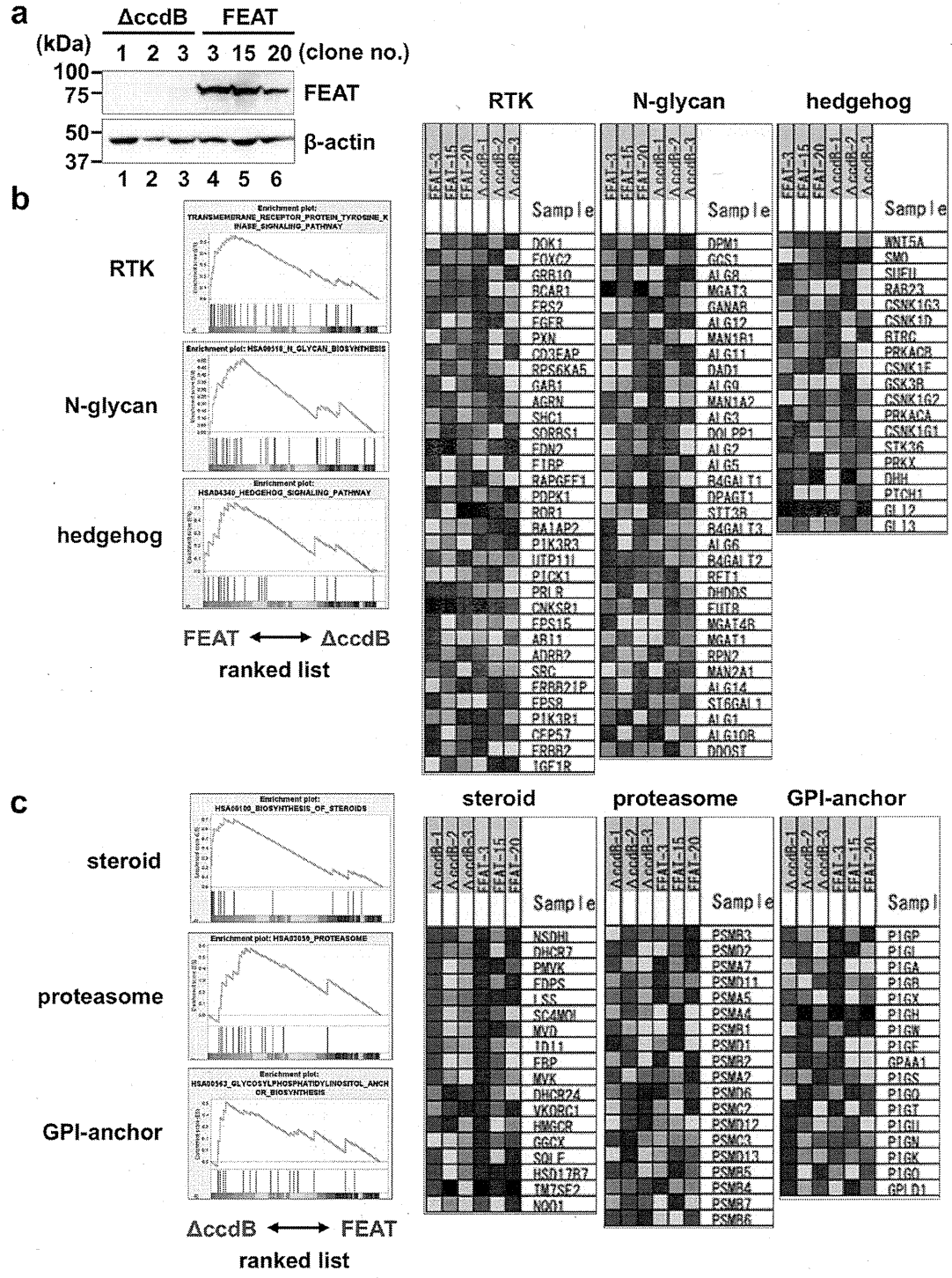

Figure 6 | Genome-wide expression profiling of NIH3T3 cells overexpressing human FEAT. (a) Immunoblot analyses of NIH3T3 cell clones stably transfected with a control plasmid (ΔccdB-1, ΔccdB-2, and ΔccdB-3) and human FEAT cDNA (FEAT-3, FEAT-15, and FEAT-20). The blot was probed with anti-FEATΔN (upper panel) and anti-actin (lower panel) antibodies. Signatures enriched in FEAT-overexpressing (FEAT-3, -15, and -20) (b) or control (ΔccdB-1, -2, and -3) (c) NIH3T3 cells as assessed by gene set enrichment analysis. Enrichment plots (left panels) and heat maps (right panels) display gene sets with enrichment score (ES) > 0.5 and false discovery rate (FDR) q-value < 0.25. RTK, receptor tyrosine kinase. GPI, glycosylphosphatidylinositol.

human *METTL13* gene at 1q24.3. These observations might explain how FEAT protein is upregulated in tumours. Further studies are needed to fully elucidate the regulation of FEAT expression in normal and neoplastic tissues.

FEAT was originally purified from rat livers as a protein that inhibits nuclear apoptosis *in vitro*. Interestingly, FEAT homologues were not detectable in unicellular eukaryotes such as yeasts and green algae (*Chlamydomonas reinhardtii*), suggesting that the functions of

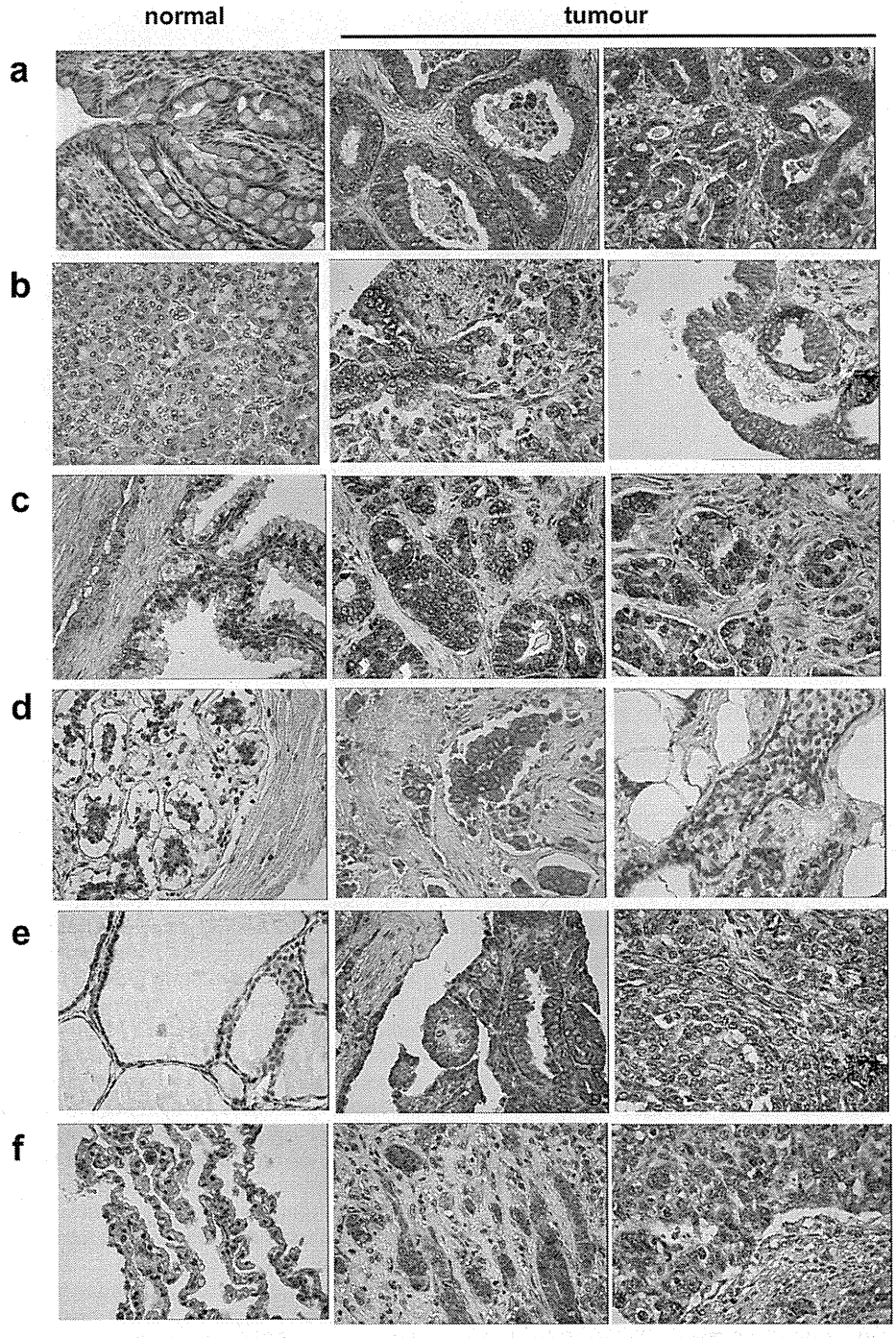

Figure 7 | Overexpression of FEAT in diverse human cancer cells. Immunohistochemical staining of Tissue Arrays using anti-FEAT ΔN antibody. (a) Normal colon tissue, grade I and III adenocarcinoma of the colon. (b) Normal pancreas tissue, grade I and II adenocarcinoma of the pancreas. (c) Normal prostate tissue, Gleason score 1 and 3 adenocarcinoma of the prostate. (d) Normal breast tissue, infiltrating ductal and lobular carcinomas of the breast. (e) Normal thyroid tissue, grade I papillary and grade III follicular carcinomas of the thyroid. (f) Normal lung tissue, grade III adenocarcinoma and grade III squamous cell carcinoma of the lung. Original magnification: × 400. The following Tissue Arrays were used: High density multiple organ cancer and normal tissue microarray, MC5001; Breast cancer tissue microarray with self-matching adjacent normal tissue and normal tissue controls, BR721; Colon adenocarcinoma (combination of marginal and normal), BC05021; and Liver carcinoma (combination of cancer, cancer adjacent and normal tissue), LV803.

FEAT are unique to multicellular organisms. Interestingly, mouse FEAT belongs to the Myc module in mouse ESCs that is responsible for the similarity between ESCs and cancer cells [53], implicating FEAT as a link between cancer and stem cell biology. *Ex vivo* experiments confirmed that FEAT attenuates apoptotic cell death. However, gene expression profiling revealed that FEAT also affects various cell signalling and metabolic pathways (Fig. 6b and 6c; Supplementary Table 2). Furthermore, in a recent genome-wide linkage analysis, genetic variations in the human *METTL13* gene have been associated with increased susceptibility to postpartum mood syndrome [54]. CpG-island microarray analyses of frontal cortex tissues have revealed higher DNA methylation close to the *METTL13* gene among bipolar

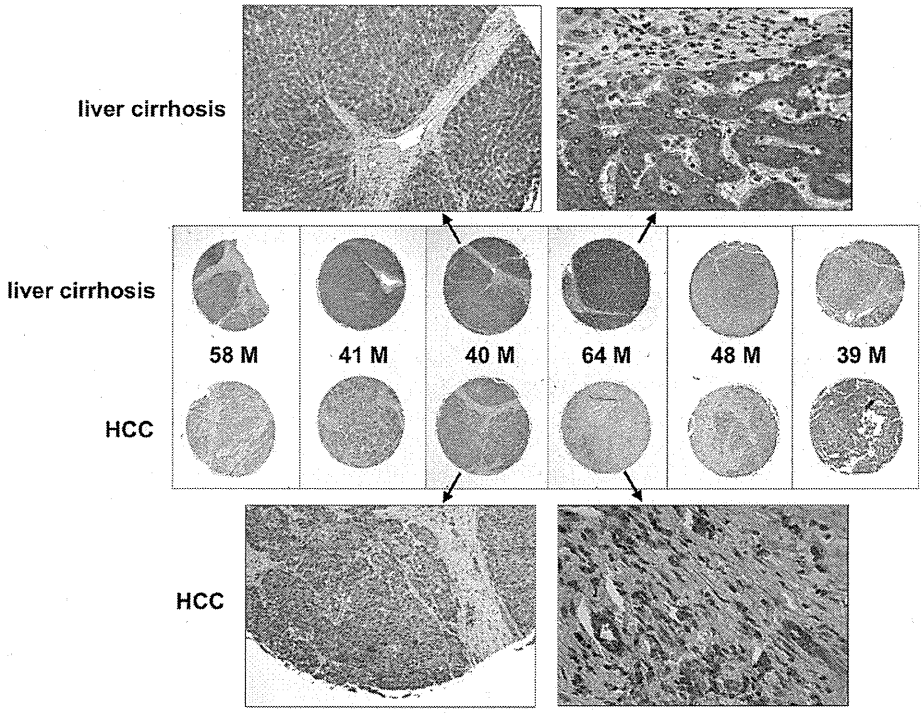

Figure 8 | FEAT is overexpressed in liver cirrhosis adjacent to human hepatocellular carcinoma (HCC). FEAT expression in HCC and the adjacent cirrhotic liver was compared for several patients using a Tissue Array (LV803). The age and gender (M, male) of the patients are indicated. Original magnifications are: ×115 (left uppermost panel, left lowermost panel), ×400 (right uppermost panel, right lowermost panel), and ×40 (middle panels).

disorder females and psychosis females [55]. Therefore, it will be important to perform integrated studies to fully elucidate how the multifunctional properties of FEAT contribute to tumorigenesis.

A potential problem with transgenic mouse models of cancer is that the transgene is expressed throughout the entire organ, while human cancers are thought to develop from a single mutated cell in the context of a relatively normal organ [32]. FEAT transgenic mice did not have the premalignant lesions (ex. steatohepatitis, cholestatic hepatitis, and liver fibrosis) that typically precede HCCs in other mouse models and human patients with underlying hepatitis B or C virus infections, alcoholic liver injury, or nonalcoholic steatohepatitis [41]. Thus, a possible limitation of the FEAT transgenic mouse model is that it cannot recapitulate the inflammatory mechanisms that underlie most human HCCs. Inflammatory responses leading to STAT3 signalling downstream of interleukin-6 have been implicated in the development of murine and human HCCs [33]. Whereas FEAT induces malignant HCCs in mice that can metastasize to the lung, constitutive interleukin-6-STAT3 signalling can only induce benign hepatic adenomas [56], suggesting that the inflammatory mechanisms play central roles mainly at earlier phases in the evolution of HCCs. Immunohistochemical analyses of Tissue Arrays from human patients revealed that FEAT is diffusely overexpressed in hepatocytes in liver cirrhosis adjacent to HCC. FEAT upregulation in transgenic mice may bypass the preneoplastic processes that precede advanced liver cirrhosis. In compensation for the inability to recapitulate the earlier inflammatory phases of hepatocarcinogenesis, FEAT transgenic mice may help us investigate a 'pure' later phase of carcinogenic processes that are not complicated by genetic alterations that are secondary to the preceding processes [57].

The relatively delayed development of HCC and lymphoma in transgenic mice (Supplementary Fig. 6) implies that FEAT is involved in promoting, rather than initiating oncogenesis. The genomic instability that was indicated by the array-CGH also suggests that multiple additional genetic alterations are required for tumorigenesis. The incidence of tumours in transgenic mouse lines was not correlated with differences in FEAT transgene expression among these lines ($1 > 16 > 23 \gg 18$), suggesting that the level of FEAT protein is not a rate-limiting factor in tumorigenesis. In addition, Tissue Arrays showed no correlation between FEAT levels and tumour grades. Downregulation of FEAT in human HCC compared to the adjacent cirrhotic liver and the moderate ability of FEAT to attenuate apoptotic cell death in HeLa cells suggested that FEAT is not necessary to maintain cancers. Taken together, these results indicate that FEAT upregulation potently promotes the development of multiple tumours *in vivo*, mainly at the prodromal and early phases of carcinogenesis, and sets the stage for additional oncogenic processes. Spontaneous lymphoma, HCC, lung cancer, and rhabdomyosarcoma can occur in C57BL/6 mice, albeit at low rates. The occurrence of these specific types of tumours suggests that the FEAT transgene promoted the intrinsic tendency of C57BL/6 mice to develop tumours such as lymphoma. Therefore, it is likely that FEAT accelerates and enhances the intrinsic predispositions of certain humans to develop cancers.

Biochemical events that are common among cancers have been used to screen or monitor tumour development, spread, and viability, as exemplified by positron emission tomography (PET) for glucose uptake. Compared to alterations in other oncogenes and tumour suppressor genes [15], FEAT is upregulated in an unusually wide range of tumours. Moreover, Tissue Array analyses demonstrate that FEAT upregulation can be easily examined using formalin-fixed paraffin-embedded sections that are available in most community hospitals. MUC1 [58] and survivin [59], which are overexpressed in diverse cancers, are currently being examined as targets for immunotherapy in clinical trials. Immunization with FEAT may trigger immune responses that eradicate precancerous lesions and early-stage tumours, preventing further development of invasive and metastatic cancers. Thus, FEAT might become the prototype of a subfamily of cancer genes that could lead to new methods for cost-effective cancer screening and prevention. The results of our study suggest that we should further explore FEAT-like ubiquitous

oncoproteins and exploit the molecular features of these proteins in various clinical applications.

Methods

Reagents. Benzyloxycarbonyl-Val-Ala-Asp(OMe)-fluoromethylketone (zVAD-fmk) was obtained from Enzyme Systems. The pcDL-SRα-procaspase-3 plasmid was kindly provided by Dr. Fumiko Toyoshima-Morimoto (Institute for Virus Research, Kyoto University, Kyoto, Japan). The agonistic anti-Fas IgM monoclonal antibody (CH-11) was purchased from MBL. The INSTA-Blot membrane (IMB-105) was obtained from IMGENEX. Multiple Tissue Blot (Human) (WB46) and Human Tumor Tissue Blot (WB51) were obtained from Calbiochem (Merck). Tissue Arrays that were spotted with an array of formalin-fixed and paraffin-embedded specimens derived from various normal and tumour tissues were purchased from US Biomax.

Antibodies. The following primary antibodies were used: rabbit polyclonal antibodies against actin (A5060; Sigma), human c-Myc (Anti-Myc Tag, 06-549; Upstate, Millipore), albumin (A0001; DakoCytomation Denmark A/S), and prosurfactant protein C (AB3786; Chemicon International, Millipore); mouse monoclonal antibodies against human c-Myc (9E10; sc-40), HA (Y-11; sc-805), MDM2 (sc-965) (Santa Cruz Biotechnology), α-fetoprotein (AB3786; Vector Laboratories), and ß-catenin (610153; BD Transduction Laboratories, BD Biosciences).

Rabbit polyclonal antibodies against human FEATΔN and human FEATΔC were produced and affinity-purified by Operon Biotechnologies (Tokyo, Japan). Detailed characterization of the antibodies is described in Supplementary Methods.

Determination of caspase cleavage sites. The candidate aspartic acid residues encoded by FEAT cDNA in the pBluescript SK(-) plasmid (Stratagene) were mutated to alanine using the GeneEditor *in vitro* Site-Directed Mutagenesis System (Promega). *In vitro* transcription/translation of the cDNAs was performed using the TNT T7/T3 Coupled Reticulocyte Lysate System (Promega) and Tran^{35}S-label (MP Biomedicals). The [^{35}S]-labelled recombinant wild-type or mutant FEAT proteins were incubated with purified recombinant caspase-3 for 2 h at 37°C, resolved by sodium dodecyl sulphate polyacrylamide gel electrophoresis (SDS-PAGE), and visualized by autoradiography.

Isolation of neutrophils, protein transduction, and analysis of spontaneous apoptosis. The PTD-4 sequence (YARAAARQARA) optimized for protein transduction [60] was introduced between the His-tag and N-terminus of the wild-type or mutant FEAT proteins. The proteins encoded by the pET-16b plasmids (Novagen, Merck) were expressed in BL21(DE3)pLys *Escherichia coli* (Novagen, Merck) and purified with Ni^{2+}-NTA agarose (Qiagen) under denaturing conditions.

Neutrophils were isolated from the peripheral blood of healthy adult volunteers using two-step Percoll (GE Healthcare Bio-Sciences) gradients. Neutrophils were resuspended in RPMI-1640 medium (Sigma) supplemented with 10% FBS (GIBCO, Invitrogen, Life Technologies), 50 U/ml penicillin, and 50 μg/ml streptomycin (GIBCO, Invitrogen, Life Technologies) (FBS-RPMI) and then treated with 1 μM of the purified proteins for 15 min at 37°C. After the treatment, the cells were diluted with FBS-RPMI and then incubated for 24 h at 37°C. Neutrophil apoptosis was assessed by ethanol fixation, propidium iodide staining, and analyses of the cells with hypodiploid DNA content using the FACScan flow cytometer and CellQuest software (BD Biosciences). Cell death was also confirmed by flow cytometric analyses of cells stained with fluorescein isothiocyanate-conjugated (FITC-conjugated) annexin V and propidium iodide using the ApoAlert annexin V Apoptosis Detection kit (Clontech Laboratories, Takara Bio).

Generation and breeding of FEAT transgenic mice. All animal experiments were approved by the Animal Experiment Committee at the Chiba Cancer Center. Injection of the DNA fragment containing the H-2K^d (MHC Class I) promoter, FEAT cDNA, β-globin intron, and SV40 poly (A) signal into fertilized eggs collected from superovulated C57BL/6CrSlc females, implantation into pseudo-pregnant mice, breeding, and weaning were performed by Japan SLC (Shizuoka, Japan).

The founder mice were screened for integration of human FEAT cDNA by Southern blotting using genomic DNA purified from tails. Briefly, 0.5 cm of mouse tails were incubated overnight at 55°C in 0.5 ml lysis buffer (10 mM TrisHCl, pH 7.5, 50 mM ethylenediamine tetraacetic acid (EDTA), 0.5% SDS, 100 mM NaCl, and 100 μg/ml proteinase K). After adding 0.5 ml UltraPure phenol:chloroform:isoamyl alcohol (Invitrogen, Life Technologies), the samples were rotated for 30 min at room temperature, and then centrifuged for 2 min at 7,000 rpm. The aqueous phase was recovered and treated similarly with 0.5 ml chloroform. The genomic DNA was precipitated by adding 0.4 ml isopropanol, and then washed with 70% ethanol and dissolved in 0.2 ml TE buffer (10 mM TrisHCl, pH 8.0, and 1 mM EDTA). After digesting with *Bam*HI and capillary transfer to Nytran SuPerCharge nylon membranes using the TurboBlotter Rapid Downward Transfer Systems (Schleicher & Schuell Bioscience, Whatman, GE Healthcare Bio-Sciences), the integrated cDNA was detected using the AlkPhos Direct Labeling and Detection System (GE Healthcare Bio-Sciences).

Thereafter, expression of the transgene in each mouse was determined by polymerase chain reaction (PCR) analysis using DNA isolated from the tail by a simplified protocol. Briefly, 0.5 cm of tail was incubated overnight at 55°C in 100 μl lysis buffer (20 mM TrisHCl, pH 7.5, 100 mM EDTA, 0.5% Tween-20 (Bio-Rad), and 100 μg/ml proteinase K), followed by the addition of 900 μl distilled water. For a 20 μl PCR reaction using KOD Dash DNA polymerase (TOYOBO), 0.5 μl of the lysate was used as a template with the following primers: 5′-TGGCTCTTTGGCATGGATGA-3′ (forward) and 5′-TATGACATCGTAGCAAGGCC-3′ (reverse). Sperm were obtained from the epididymides of transgenic mice and cryopreserved by Kyudo Co., Ltd. (Tosu, Japan).

Transgenic mice and their nontransgenic littermates were bred and maintained in a specific pathogen-free (SPF) animal facility at the Chiba Cancer Center Research Institute. Transgenic lines were maintained by crossing male transgenic mice to normal female C57BL/6 mice (Charles River Laboratories). Mice that had tumours or were in a moribund state were euthanized and necropsied.

Apoptotic cell death of mouse thymocytes. Thymocytes were isolated by grinding the dissected thymus with the plunger of a 1-ml sterile syringe in FBS-RPMI at room temperature. The cells were left untreated or treated with Fas ligand (rhs*Super*FasLigand) (Alexis) or dexamethasone (Nacalai Tesque) for 24 h at 37°C in a humidified atmosphere containing 5% CO_2. Cell death was quantified by staining the cells with annexin V-CFS (R&D Systems) and propidium iodide (Calbiochem, Merck), and then analyzing the cells by flow cytometry.

Microscopic analyses of mouse tissues. After dissection, the mouse organs were fixed with 3.7% formaldehyde in phosphate-buffered saline, sliced into 2-mm thick sections, placed into tissue cassettes (Tissue-Tek Uni-Cassette; Sakura Finetek Japan), and immersed in fresh fixative. Further processing and interpretation of the microscopic pathology were performed by Narabyouri Research Co., Ltd. (Nara, Japan). Briefly, fixed tissues were dehydrated through a series of ethanol (20% to 100%) and xylene solutions and embedded in paraffin using an automatic tissue processor, sectioned with a microtome, deparaffinized, rehydrated, and stained with hematoxylin and eosin (H&E). Immunohistochemical staining for CD45R (B220) and CD3 was performed with an Autostainer (DAKO).

Array-CGH. The quality of genomic DNA was assessed by electrophoresis of 200 ng DNA on a 0.8% agarose gel containing 0.5 μg/ml ethidium bromide. Only DNA preparations without smearing were used for subsequent steps. DNA labelling and hybridization to 244k slide format 60-mer oligonucleotide microarrays for array-CGH (Agilent Mouse Genome CGH Microarray Kit 244A) were performed using genomic DNA from mouse HCCs as experimental samples and genomic DNA from the liver of a normal C57BL/6 mouse as a reference sample. The microarrays were scanned using a Micro Array Scanner, and data were extracted using Feature Extraction software and analyzed using CGH analytics 3.4 software according to the manufacturer's instructions (Agilent Technologies).

Gene expression profiling with microarrays. The ORF of human FEAT cDNA was subcloned into the pEF-DEST51 vector (Invitrogen, Life Technologies). NIH3T3 cells were transfected with pEF-DEST51-FEAT using HilyMax (Dojindo Laboratories). After 7 days of selection with 10 μg/ml blasticidin S (Kaken Pharmaceutical), colonies were picked and screened for clones in which FEAT protein was overexpressed. The *ccdB* gene in the pEF-DEST51 vector was deleted to construct the pEF-DEST51-ΔccdB plasmid, which was stably transfected into NIH3T3 cells to obtain control cell lines.

Total RNA was extracted from control (ΔccdB-1, -2, and -3) and FEAT-overexpressing NIH3T3 cell lines (FEAT-3, -15, and -20) using the RNeasy Mini kit (Qiagen). Gene expression profiling was performed with Sentrix Mouse WG-6 v2 BeadChip Array (Illumina) at the Research Support Center, Graduate School of Medical Sciences, Kyushu University. Raw gene expression data were first subjected to average normalization using BeadStudio 3.0 software. Average signals with detection *P*-values (based on Illumina replicate gene probes) > 0.01 were removed from analyses. GSEA was performed using the software available via the world wide web site (http://www.broadinstitute.org/gsea/).

Immunohistochemistry. Paraffin-embedded sections were deparaffinized with Clear-Advantage (Polysciences), rehydrated, treated with Citrate-based Antigen Unmasking Solution (Vector Laboratories), and stained using the ImmPRESS kit (Vector Laboratories) and ImmPACT Chromogen (Vector Laboratories) according to the manufacturer's instructions. The slides were counterstained with Mayer's Hematoxylin (Merck), and the coverslips were mounted with Gel/Mount aqueous mounting medium (Biomeda). The stained tissues were observed by the Zeiss Axioskop 2 *plus* microscope and images were acquired using the Zeiss AxioCam camera controlled by AxioVision software (Carl Zeiss MicroImaging). Images were also captured using the Leica MZ16 FA stereomicroscope, Leica DFC300 FX digital camera, and Leica IM500 Image Manager software (Leica Microsystems).

1. Bode, A. M. & Dong, Z. Cancer prevention research - then and now. *Nat. Rev. Cancer* **9**, 508–516 (2009).
2. Futreal, P. A. *et al.* A census of human cancer genes. *Nat. Rev. Cancer* **4**, 177–183 (2004).
3. Sjoblom, T. *et al.* The consensus coding sequences of human breast and colorectal cancers. *Science* **314**, 268–274 (2006).
4. Greenman, C. *et al.* Patterns of somatic mutation in human cancer genomes. *Nature* **446**, 153–158 (2007).
5. Wood, L. D. *et al.* The genomic landscapes of human breast and colorectal cancers. *Science* **318**, 1108–1113 (2007).

6. Jones, S. *et al.* Core signaling pathways in human pancreatic cancers revealed by global genomic analyses. *Science* **321**, 1801–1806 (2008).
7. Parsons, D. W. *et al.* An integrated genomic analysis of human glioblastoma multiforme. *Science* **321**, 1807–1812 (2008).
8. The Cancer Genome Atlas Research Network. Comprehensive genomic characterization defines human glioblastoma genes and core pathways. *Nature* **455**, 1061–1068 (2008).
9. Ding, L. *et al.* Somatic mutations affect key pathways in lung adenocarcinoma. *Nature* **455**, 1069–1075 (2008).
10. van der Brug, M. P. & Wahlestedt, C. Navigating genomic maps of cancer cells. *Nat. Biotechnol.* **28**, 241–242 (2010).
11. Meyerson, M., Gabriel, S. & Getz, G. Advances in understanding cancer genomes through second-generation sequencing. *Nat. Rev. Genet.* **11**, 685–696 (2010).
12. Stephens, P. J. *et al.* Complex landscapes of somatic rearrangement in human breast cancer genomes. *Nature* **462**, 1005–1010 (2009).
13. Stratton, M. R., Campbell, P. J. & Futreal, P. A. The cancer genome. *Nature* **458**, 719–724 (2009).
14. Hanahan, D. & Weinberg, R. A. Hallmarks of cancer: the next generation. *Cell* **144**, 646–674 (2011).
15. Vogelstein, B. & Kinzler, K. W. Cancer genes and the pathways they control. *Nat. Med.* **10**, 789–799 (2004).
16. Vander Heiden, M. G., Cantley, L. C. & Thompson, C. B. Understanding the Warburg effect: the metabolic requirements of cell proliferation. *Science* **324**, 1029–1033 (2009).
17. Shamji, A. F., Nghiem, P. & Schreiber, S. L. Integration of growth factor and nutrient signaling: implications for cancer biology. *Mol. Cell* **12**, 271–280 (2003).
18. Luo, J., Solimini, N. L. & Elledge, S. J. Principles of cancer therapy: oncogene and non-oncogene addiction. *Cell* **136**, 823–837 (2009).
19. Hanahan, D., Wagner, E. F. & Palmiter, R. D. The origins of oncomice: a history of the first transgenic mice genetically engineered to develop cancer. *Genes Dev.* **21**, 2258–2270 (2007).
20. Santarius, T., Shipley, J., Brewer, D., Stratton, M. R. & Cooper, C. S. A census of amplified and overexpressed human cancer genes. *Nat. Rev. Cancer* **10**, 59–64 (2010).
21. Lazebnik, Y. A., Cole, S., Cooke, C. A., Nelson, W. G. & Earnshaw, W. C. Nuclear events of apoptosis in vitro in cell-free mitotic extracts: a model system for analysis of the active phase of apoptosis. *J. Cell Biol.* **123**, 7–22 (1993).
22. Takahashi, A. *et al.* Cleavage of lamin A by Mch2 alpha but not CPP32: multiple interleukin 1 beta-converting enzyme-related proteases with distinct substrate recognition properties are active in apoptosis. *Proc. Natl. Acad. Sci. USA* **93**, 8395–8400 (1996).
23. Lai, C. H., Chou, C. Y., Ch'ang, L. Y., Liu, C. S. & Lin, W. Identification of novel human genes evolutionarily conserved in *Caenorhabditis elegans* by comparative proteomics. *Genome Res.* **10**, 703–713 (2000).
24. Kagan, R. M. & Clarke, S. Widespread occurrence of three sequence motifs in diverse S-adenosylmethionine-dependent methyltransferases suggests a common structure for these enzymes. *Arch. Biochem. Biophys.* **310**, 417–427 (1994).
25. Wirsing, L., Naumann, K. & Vogt, T. Arabidopsis methyltransferase fingerprints by affinity-based protein profiling. *Anal. Biochem.* **408**, 220–225 (2011).
26. Janicke, R. U., Sprengart, M. L., Wati, M. R. & Porter, A. G. Caspase-3 is required for DNA fragmentation and morphological changes associated with apoptosis. *J. Biol. Chem.* **273**, 9357–9360 (1998).
27. Kurokawa, M. & Kornbluth, S. Caspases and kinases in a death grip. *Cell* **138**, 838–854 (2009).
28. Schwarze, S. R., Hruska, K. A. & Dowdy, S. F. Protein transduction: unrestricted delivery into all cells? *Trends Cell Biol.* **10**, 290–295 (2000).
29. Velculescu, V. E. *et al.* Analysis of human transcriptomes. *Nat. Genet.* **23**, 387–388 (1999).
30. Naugler, W. E. *et al.* Gender disparity in liver cancer due to sex differences in MyD88-dependent IL-6 production. *Science* **317**, 121–124 (2007).
31. Anisimov, V. N., Ukraintseva, S. V. & Yashin, A. I. Cancer in rodents: does it tell us about cancer in humans? *Nat. Rev. Cancer* **5**, 807–819 (2005).
32. Frese, K. K. & Tuveson, D. A. Maximizing mouse cancer models. *Nat. Rev. Cancer* **7**, 645–658 (2007).
33. Grivennikov, S. I., Greten, F. R. & Karin, M. Immunity, inflammation, and cancer. *Cell* **140**, 883–899 (2010).
34. Hussain, S. P., Schwank, J., Staib, F., Wang, X. W. & Harris, C. C. TP53 mutations and hepatocellular carcinoma: insights into the etiology and pathogenesis of liver cancer. *Oncogene* **26**, 2166–2176 (2007).
35. Toledo, F. & Wahl, G. M. Regulating the p53 pathway: in vitro hypotheses, in vivo veritas. *Nat. Rev. Cancer* **6**, 909–923 (2006).
36. Laurent-Puig, P. & Zucman-Rossi, J. Genetics of hepatocellular tumors. *Oncogene* **25**, 3778–3786 (2006).
37. Zender, L. *et al.* Identification and validation of oncogenes in liver cancer using an integrative oncogenomic approach. *Cell* **125**, 1253–1267 (2006).
38. Latres, E. *et al.* Role of the F-box protein Skp2 in lymphomagenesis. *Proc. Natl. Acad. Sci. USA* **98**, 2515–2520 (2001).
39. Clancy, J. L. *et al.* EDD, the human orthologue of the hyperplastic discs tumour suppressor gene, is amplified and overexpressed in cancer. *Oncogene* **22**, 5070–5081 (2003).
40. Graham, M. & Adams, J. M. Chromosome 8 breakpoint far 3′ of the c-myc oncogene in a Burkitt's lymphoma 2;8 variant translocation is equivalent to the murine pvt-1 locus. *EMBO J.* **5**, 2845–2851 (1986).
41. Farazi, P. A. & DePinho, R. A. Hepatocellular carcinoma pathogenesis: from genes to environment. *Nat. Rev. Cancer* **6**, 674–687 (2006).
42. Chin, L. & Gray, J. W. Translating insights from the cancer genome into clinical practice. *Nature* **452**, 553–563 (2008).
43. Subramanian, A. *et al.* Gene set enrichment analysis: a knowledge-based approach for interpreting genome-wide expression profiles. *Proc. Natl. Acad. Sci. USA* **102**, 15545–15550 (2005).
44. Gschwind, A., Fischer, O. M. & Ullrich, A. The discovery of receptor tyrosine kinases: targets for cancer therapy. *Nat. Rev. Cancer* **4**, 361–370 (2004).
45. Rubin, L. L. & de Sauvage, F. J. Targeting the Hedgehog pathway in cancer. *Nat. Rev. Drug Discov.* **5**, 1026–1033 (2006).
46. Varjosalo, M. & Taipale, J. Hedgehog: functions and mechanisms. *Genes Dev.* **22**, 2454–2472 (2008).
47. Kim, B. *et al.* Expression profiling and subtype-specific expression of stomach cancer. *Cancer Res.* **63**, 8248–8255 (2003).
48. Gratias, S. *et al.* Genomic gains on chromosome 1q in retinoblastoma: consequences on gene expression and association with clinical manifestation. *Int. J. Cancer* **116**, 555–563 (2005).
49. Vincent-Salomon, A. *et al.* Integrated genomic and transcriptomic analysis of ductal carcinoma in situ of the breast. *Clin. Cancer Res.* **14**, 1956–1965 (2008).
50. Kim, J., Chu, J., Shen, X., Wang, J. & Orkin, S. H. An extended transcriptional network for pluripotency of embryonic stem cells. *Cell* **132**, 1049–1061 (2008).
51. Chen, X. *et al.* Integration of external signaling pathways with the core transcriptional network in embryonic stem cells. *Cell* **133**, 1106–1117 (2008).
52. Liu, X. *et al.* Yamanaka factors critically regulate the developmental signaling network in mouse embryonic stem cells. *Cell Res.* **18**, 1177–1189 (2008).
53. Kim, J. *et al.* A Myc network accounts for similarities between embryonic stem and cancer cell transcription programs. *Cell* **143**, 313–324 (2010).
54. Mahon, P. B. *et al.* Genome-wide linkage and follow-up association study of postpartum mood symptoms. *Am. J. Psychiatry* **166**, 1229–1237 (2009).
55. Mill, J. *et al.* Epigenomic profiling reveals DNA-methylation changes associated with major psychosis. *Am. J. Hum. Genet.* **82**, 696–711 (2008).
56. Rebouissou, S. *et al.* Frequent in-frame somatic deletions activate gp130 in inflammatory hepatocellular tumours. *Nature* **457**, 200–204 (2009).
57. Thorgeirsson, S. S. & Grisham, J. W. Molecular pathogenesis of human hepatocellular carcinoma. *Nat. Genet.* **31**, 339–346 (2002).
58. Kufe, D. W. Mucins in cancer: function, prognosis and therapy. *Nat. Rev. Cancer* **9**, 874–885 (2009).
59. Altieri, D. C. Survivin, cancer networks and pathway-directed drug discovery. *Nat. Rev. Cancer* **8**, 61–70 (2008).
60. Ho, A., Schwarze, S. R., Mermelstein, S. J., Waksman, G. & Dowdy, S. F. Synthetic protein transduction domains: enhanced transduction potential in vitro and in vivo. *Cancer Res.* **61**, 474–477 (2001).

Acknowledgements

We thank T. Honjo, I. Chung-Okazaki, A. Shirahata, T. Hashimoto, C. F. Clarke, P. Gin, W. Frommer, X. Wang, F. Toyoshima-Morimoto, and A. K. Munirajan for reagents; H. Ohno for cell lines; M. Sugimoto, K. Igarashi, and the Research Support Center, Graduate School of Medical Sciences, Kyushu University for technical support; S. H. Kaufmann, T. Marumoto, and A. Suzuki for critically reading; K. Sakurai, Y. Nakamura, N. Shibano-Kondo, A. Kitabayashi-Akao, S. Ito, and M. Okada for technical assistance; T. Moriguchi, M. Taketo, T. Hori, T. Ichinohe, K. Yamamoto, M. Sasada, T. Uchiyama, A. Uemura, A. Kotani-Yoshida, T. Ozaki, H. Kageyama, S. Haraguchi, M. Mizoe-Amako, T. Nakamura, and E. Nishida for discussions and suggestions; J. Hirai, Y. Asano-Ashida, K. Miyata, M. Ushijima, and K. Maekawa for secretarial assistance. This work was supported by Grants-in-Aid from the Ministry of Education, Culture, Sports, Science, and Technology of Japan, the Academic Research Grant from Kyoto University, and a grant from the Tokyo Biochemical Research Foundation.

Author contributions

AT designed the project. AT, DT, AN, and KTani designed experiments. AT, HT, KTakahashi, TT, KM, AI, OK, and KY performed a significant amount of the experimental work. AT, MO, and TK performed most of the data collection and data analysis. AT wrote the main manuscript text and prepared figures and tables. All authors reviewed the manuscript.

Additional information

Supplementary Information accompanies this paper at http://www.nature.com/scientificreports

Author Information Human FEAT cDNAs are deposited in GenBank (AB242174 and AB242175). Microarray data are deposited in GEO (expression microarray, GSE18299; array-CGH, GSE18403).

Competing financial interests: The authors declare no competing financial interests.

How to cite this article: Takahashi, A. *et al.* A novel potent tumour promoter aberrantly overexpressed in most human cancers. *Sci. Rep.* 1, 15; DOI:10.1038/srep00015 (2011).

Published OnlineFirst March 29, 2012; DOI:10.1158/0008-5472.CAN-11-3185

Cancer Research

Coxsackievirus B3 Is an Oncolytic Virus with Immunostimulatory Properties That Is Active against Lung Adenocarcinoma

Shohei Miyamoto, Hiroyuki Inoue, Takafumi Nakamura, et al.

Cancer Res 2012;72:2609-2621. Published OnlineFirst March 29, 2012.

Published OnlineFirst March 29, 2012; DOI:10.1158/0008-5472.CAN-11-3185

Therapeutics, Targets, and Chemical Biology

Cancer Research

Coxsackievirus B3 Is an Oncolytic Virus with Immunostimulatory Properties That Is Active against Lung Adenocarcinoma

Shohei Miyamoto[1], Hiroyuki Inoue[1,2], Takafumi Nakamura[3], Meiko Yamada[4], Chika Sakamoto[1], Yasuo Urata[4], Toshihiko Okazaki[1], Tomotoshi Marumoto[1], Atsushi Takahashi[1], Koichi Takayama[2], Yoichi Nakanishi[2], Hiroyuki Shimizu[5], and Kenzaburo Tani[1]

Abstract

Although oncolytic virotherapy is a promising anticancer therapy, antitumor efficacy is hampered by low tumor selectivity. To identify a potent and selective oncolytic virotherapy, we carried out large-scale two-step screening of 28 enteroviral strains and found that coxsackievirus B3 (CVB3) possessed specific oncolytic activity against nine human non–small cell lung cancer (NSCLC) cell lines. CVB3-mediated cytotoxicity was positively correlated with the expression of the viral receptors, coxsackievirus and adenovirus receptor, and decay-accelerating factor, on NSCLC cells. *In vitro* assays revealed that the CVB3 induced apoptosis and phosphoinositide 3-kinase/Akt and mitogen-activated protein (MAP)/extracellular signal-regulated (ERK) kinase (MEK) survival signaling pathways, leading to cytotoxicity and regulation of CVB3 replication. Intratumoral injections of CVB3 elicited remarkable regression of preestablished NSCLC tumors *in vivo*. Furthermore, administrations of CVB3 into xenografts on the right flank resulted in significantly durable regression of uninjected xenografts on the left flank, where replication-competent CVB3 was detected. All treatments with CVB3 were well tolerated without treatment-related deaths. In addition, after CVB3 infection, NSCLC cells expressed abundant cell surface calreticulin and secreted ATP as well as translocated extranuclear high-mobility group box 1, which are required for immunogenic cell death. Moreover, intratumoral CVB3 administration markedly recruited natural killer cells and granulocytes, both of which contributed to the antitumor effects as shown by depletion assays, macrophages, and mature dendritic cells into tumor tissues. Together, our findings suggest that CVB3 is a potent and well-tolerated oncolytic agent with immunostimulatory properties active against both localized and metastatic NSCLC. *Cancer Res; 72(10); 2609–21. ©2012 AACR.*

Introduction

Oncolytic viruses are self-replicating, tumor-selective viruses, with an ability to directly induce cancer cell death, and have emerged as a promising treatment platform for cancer therapy (1).

Over the past 2 decades, clinical trials of oncolytic virotherapies using a range of DNA and RNA viruses including coxsackievirus A21 (CVA21), measles virus, Newcastle disease virus, and reovirus have been reported or are underway (2–5). Clinical development of these therapies has progressed to late phase trials. However, the antitumor efficacy of oncolytic viruses has yet to attain the potential anticipated in preclinical studies.

RNA viruses seem to be a safer modality, as most single-stranded RNA viruses replicate in the host cytosol without a DNA phase. Therefore, they lack the genotoxicity caused by integration of the viral genome into the host DNA. In particular, enteroviruses, members of the *Picornaviridae* family, a diverse group of small RNA viruses have emerged as promising candidates for cancer treatment (6–9). Their use has several therapeutic advantages: these viruses immediately induce robust cytolytic changes during cell-to-cell infection, they do not possess oncogenes that may lead to tumorigenesis, and they can be easily genetically manipulated by reverse genetics systems for the rescue of positive-strand RNA viruses from complementary DNA (10, 11). Furthermore, most nonpolio enteroviruses are common and highly prevalent and are mainly associated with asymptomatic infection or mild disease (12). Although CVA21 is reportedly a potent oncolytic enterovirus against

Authors' Affiliations: [1]Division of Molecular and Clinical Genetics, Medical Institute of Bioregulation; [2]Research Institute for Diseases of the Chest, Graduate School of Medical Sciences, Kyushu University, Fukuoka; [3]Core Facility for Therapeutic Vectors, The Institute of Medical Science, The University of Tokyo; [4]Oncolys BioPharma Inc.; and [5]Department of Virology II, National Institute of Infectious Diseases, Tokyo, Japan

Note: Supplementary data for this article are available at Cancer Research Online (http://cancerres.aacrjournals.org/).

S. Miyamoto and H. Inoue contributed equally to this work.

Corresponding Author: Kenzaburo Tani, Division of Molecular and Clinical Genetics, Medical Institute of Bioregulation, Kyushu University, 3-1-1 Maidashi, Higashi-ku, Fukuoka 812-8582, Japan. Phone: 81-92-642-6449; Fax: 81-92-642-6444; E-mail: taniken@bioreg.kyushu-u.ac.jp

doi: 10.1158/0008-5472.CAN-11-3185

Published OnlineFirst March 29, 2012; DOI:10.1158/0008-5472.CAN-11-3185

miscellaneous human cancer cells (8, 9, 13), CVA21-treated mice died of lethal myositis with paralysis (14).

Apart from direct oncolysis, another important component of the sustained therapeutic advantage of oncolytic viruses depends on their ability to trigger antitumor immune responses (15). Robust viral replication in tumors provides immunologic damage-associated molecular pattern (DAMP) signals, augmenting the immunogenicity of the tumor microenvironment (16). Previous studies showed that several oncolytic viruses could induce adaptive antitumor immunity by tumor-specific CTL responses (17). However, little is known about how preceding innate immunity shapes the antitumor effects and whether oncolytic viruses cause immunogenic cancer cell death by similar mechanisms to chemotherapeutic agents, such as calreticulin (CRT) exposure, ATP release, or high-mobility group box 1 (HMGB1) translocation (18).

The focus of this study was to identify a novel oncolytic virus from screening 28 different strains of human enteroviruses, which had high tolerability when administered in mouse xenograft models, and to clarify the viral cytocidal mechanism by scrutinizing the apoptotic and antitumor immunogenic potential of the virus.

Materials and Methods

Mice

Female BALB/c nude mice were purchased from Charles River Japan. All animal experiments were carried out under the Guidelines for Animal Experiments of Kyushu University and Law 105 Notification 6 of the Japanese Government.

Cell lines

The non–small cell lung cancer (NSCLC; A549, H1299, and H460), colon cancer (Caco-2), pancreatic cancer (AsPC-1), renal cancer (A-498 and Caki-1), rhabdomyosarcoma (RD), T-cell leukemia (HuT 102), bone marrow stromal (HS-5), and normal lung fibroblast (MRC-5) cell lines were purchased from the American Type Culture Collection. NSCLC cell lines (PC-9, EBC-1, and LK-2) were obtained from the Health Science Research Resources Bank in Japan. Human lung squamous cell carcinoma cell lines (QG-56 and QG-95) were provided by Dr Y. Ichinose (National Kyushu Cancer Center; ref. 19). The other NSCLC cell lines (LK-87 and Sq-1) were obtained from Cell Resource Center for Biomedical Research, Tohoku University. Human cell lines of colon cancer (DLD-1), pancreatic cancer (PANC-1), breast cancer (MCF7), cervical cancer (HeLa S3), and normal lung fibroblast (NHLF) were provided by Dr T. Fujiwara (Okayama University). No authentication besides PCR tests that showed free from *Mycoplasma* contamination was done for all of cell lines used.

Production of enteroviruses

The 28 strains of enteroviruses tested were obtained from H. Shimizu (National Institute of Infectious Diseases, Japan) and were propagated in HeLa and RD cells. The $TCID_{50}$/mL on these cell monolayers was determined as previously described (20).

Crystal violet staining

Viable cells at 72-hour postinfection with enteroviruses at appropriate multiplicity of infection (MOI) for 1 hour were assessed by crystal violet staining as previously described (21). Cell survival rates were calculated by Multi Gauge software version 3.2 (FUJIFILM).

Flow cytometry analysis

Cells were incubated with a monoclonal antibody against coxsackievirus and adenovirus receptor (CAR; Upstate) followed by incubation with fluorescein isothiocyanate (FITC)-conjugated anti-mouse immunoglobulin G, or phycoerythrin (PE)-conjugated antibody decay-accelerating factor (DAF; BD Biosciences). For analysis of surface CRT, NSCLC cells infected with Coxsackievirus B3 (CVB3; MOI = 10) was analyzed by flow cytometric analysis (22). Data were obtained with a FACSCalibur (BD Biosciences) and analyzed by FlowJo software Version 7.6 (Tree Star Inc.).

MTS assay for cell viability

In vitro cell viability experiments using cells infected with CVB3 were carried out by a Cell Titer 96 AQueous Non-Radioactive Cell Proliferation Assay (Promega) following the manufacturer's instructions.

In vitro inhibition assays

Cells were pretreated with serum-free media containing the specific phosphoinositide 3-kinase (PI3K) inhibitor LY294002 (Santa Cruz Biotechnology), the PTEN inhibitor bisperoxovanadium (bpV, HOpic; Merck), or the mitogen-activated protein (MAP)/extracellular signal-regulated kinase (ERK; MEK) inhibitor PD0325901 (Wako) for 1 hour, and then infected with CVB3 (MOI = 10) for 1 hour. For apoptosis inhibition assay, A549 cells were pretreated with the pan-caspase inhibitor, z-VAD-fmk (100 or 200 μmol/L for 1 hour; R&D Systems), exposed to CVB3 at MOI of 0.01 or 0.1 for 1 hour, and replaced in indicated concentrations of z-VAD-fmk for additional 48 hours.

siRNA transfection assay

siRNAs specific for human CAR and a negative control were designed and synthesized by BONAC in Japan. Transfection of A549 cells with siRNAs was carried out with Lipofectamine 2000 (Invitrogen) according to the manufacturer's protocol. Following 72-hour incubation after transfection, cells were infected with CVB3 at MOI of 0.01 for MTS assays.

Western blot analysis

Cell lysate samples were resolved by SDS-PAGE and immunoblotted (21). The primary antibodies used were monoclonal antibodies against PARP (Biovision), phospho-Akt (Ser473; BioLegend), and β-actin (Santa Cruz Biotechnology). Densitometry analysis was conducted with LAS3000 (FUJIFILM) and Multi Gauge software version 3.2.

Annexin V staining and cell-cycle analysis

Apoptotic cells after CVB3 infection were determined with the Annexin V–PE apoptosis detection kit (BD Biosciences) according to the manufacturer's instructions. For cell-cycle

Published OnlineFirst March 29, 2012; DOI:10.1158/0008-5472.CAN-11-3185

analysis, the cells were fixed in 70% ethanol, incubated with RNase A (50 μg/mL), stained with 10 μg/mL propidium iodide (PI), and analyzed with a FACS-Calibur.

ATP release assay

After cell death induction, secreted extracellular ATP was measured with the luciferin-based ENLITEN ATP Assay (Promega) according to the manufacturer's protocol.

Immunofluorescence microscopy

Cells fixed with 4% paraformaldehyde were permeabilized with 0.3% Triton X-100 for 10 minutes, incubated with anti-HMGB1 antibody for 30 minutes followed by incubation with Alexa Fluor 488–conjugated secondary antibody (Molecular Probes), and analyzed by a fluorescence microscope BZ-9000 (KEYENCE).

In vivo therapeutic studies

A549 cells (5×10^6 cells) or EBC-1 cells (3×10^6 cells) were injected subcutaneously into the right or bilateral flanks of nude mice. When tumors reached diameters of 0.4 to 0.6 cm, the tumors on the right flank were inoculated with CVB3 (5×10^6 $TCID_{50}$) once on day 2 or with the same doses of CVB3 on days 2, 4, 6, 8, and 10.

The RB6-8C5 rat hybridoma cell line producing the anti-mouse Gr-1 monoclonal antibody was provided by Dr T. Yokomizo (Kyushu University). For granulocyte depletion, nude mice implanted with 5×10^6 A549 cells were intraperitoneally injected with 300 μg rat anti–Gr-1 antibody (99.7% elimination of circulating polymorphonuclear neutrophils). For natural killer (NK) cell depletion, nude mice were intraperitoneally injected with rabbit polyclonal anti-asialo GM1 antibody (Wako; ref. 23). The tumor volume was calculated as length × width × width/2 and expressed as means ± SEM. Animals were euthanized when the tumor diameter exceeded 1.0 cm.

Tumor-infiltrating lymphocytes

The excised tumors were gently homogenized with sharp syringes, incubated for 90 minutes in RPMI-1640 containing collagenase (Invitrogen). For innate immunity subpopulations, the cells were stained with anti-mouse DX-5-FITC, Gr-1-PE, F4/80-APC, or CD11c-APC antibodies for 30 minutes. For mature dendritic cells (DC), the cells were stained with anti-mouse CD86-FITC, CD80-PE, CCR7-PerCP, and CD11c-APC antibody for 30 minutes. For cytolytic effector cells, the cells were stained with anti-mouse DX-5-FITC, Gr-1-PerCP, and CD107a-PE antibody for 30 minutes (24) and analyzed by a FACS Calibur.

Statistical analyses

Statistical analyses were conducted with GraphPad Prism 5.0d software package (GraphPad Software Inc.). Statistical analysis was conducted using a 2-tailed unpaired Student *t* test, one-way ANOVA followed by Tukey multiple comparison test, or nonparametric Mann–Whitney *U* test. $P < 0.05$ was considered statistically significant. Survival curves were plotted according to the Kaplan–Meier method (log-rank test).

Results

Sequential two-step screening identifies CVB3 as a candidate for oncolytic virus against NSCLC

To identify a safer and more potent oncolytic enterovirus, we carried out a large-scale screening of 28 strains of enteroviruses for oncolytic activity. This screening was carried out *in vitro* against 12 different human cancer cell lines and the HS-5 normal bone marrow stromal cell line using crystal violet staining. Several enteroviruses displayed marked cytotoxic effects (Fig. 1A) in a dose-dependent manner (Supplementary Fig. S1A and S1B). The Coxsackievirus B group, CVB2 (Ohio-1), CVB3 (Nancy), and CVB4 (J.V.B.) were of particular interest, as they showed exclusive oncolytic effects on the A549 and LK-87 NSCLC cell lines (Fig. 1A). In a secondary screen, we evaluated the oncolytic efficacy of CVB2, CVB3, and CVB4 against 9 additional NSCLC cell lines and 2 normal lung cell lines. Unexpectedly, only CVB3 infection induced marked cytolysis in 100% (9 of 9) NSCLC cell lines of diverse histologic subtypes, that is, adenocarcinoma (A549), squamous cell carcinoma (EBC-1), and large cell carcinoma (H460) even at an MOI of 0.001. However, CVB3 did not induce cytolysis against normal lung fibroblast cell lines even at an MOI as high as 10 (Fig. 1B). Accordingly, we employed CVB3 harboring potent and specific cytolytic activity as a candidate virus for oncolytic virotherapy against NSCLC.

Correlation of CVB3-mediated cytotoxicity and expression levels of surface receptors on NSCLC Cells

We next compared the expression level of the CVB3 receptors, CAR and DAF (25) on various human NSCLC and normal lung cell lines. NSCLC cell lines expressed moderate to high levels of CAR, whereas normal lung cell lines expressed very low levels of CAR. The expression of DAF was similarly high in the NSCLC and normal lung cell lines (Fig. 2A). The oncolytic activity of CVB3 significantly correlated with a number that was equal to the percentage of CAR-expressing cells multiplied by the percentage of DAF-expressing cells ($r = -0.92$, $P < 0.0001$), whereas 2 normal lung cell lines were unaffected (Fig. 2B). The results of the *in vitro* MTS cell viability assays confirmed this correlation in a time-dependent manner (Fig. 2C). To thereby elucidate the role of CAR in the cytolytic effects of CVB3, CVB3-infected A549 cells were analyzed in the presence of siRNA-mediated functional CAR knockdown. Flow cytometric analyses confirmed the reduction of CAR expression by 92% in A549 cells transfected with CAR-specific siRNA (Supplementary Fig. S2). The inhibition of CAR significantly abrogated the cytotoxicity of CVB3 ($P < 0.001$; Fig. 2D).

Contribution of caspase-mediated apoptosis and PI3K/Akt or MEK/ERK signaling pathways to CVB3-mediated cytotoxicity in NSCLC cells

To determine whether CVB3 induced apoptosis in NSCLC cells treated with CVB3 (MOI = 0.1), we examined the cleavage of PARP by caspases, an execution marker of apoptosis. Western blot analysis revealed cleaved PARP (85 kDa) in CVB3-treated A549 and LK-2 NSCLC cells, but not in CVB3-